April 2023

Stretch Activation During Fatigue Improves Relative Force Production in Fast-Contracting Mouse Skeletal Muscle Fibers

Philip C. Woods
University of Massachusetts Amherst

Stretch Activation During Fatigue Improves Relative Force Production in Fast-Contracting Mouse Skeletal Muscle Fibers

A Thesis Presented

by

PHILIP CHRISTOPHER WOODS

Submitted to the Graduate School of the
University of Massachusetts Amherst in partial fulfillment
of the requirements for the degree of

MASTER OF SCIENCE

February 2023

Kinesiology

Stretch Activation During Fatigue Improves Relative Force Production in Fast-Contracting Mouse Skeletal Muscle Fibers

A Thesis Presented

by

Philip Christopher Woods

Approved as to style and content by:

DocuSigned by:
Mark Miller
E81B9BA93977430...

Mark S. Miller, Chair.

DocuSigned by:
Jane A. Kent
8DD63332AE0B409...

Jane A. Kent, Member.

DocuSigned by:
Edward Debold
60FD0A15A9CE401...

Edward E. Debold, Member.

DocuSigned by:
Douglas Swank
B2E2E3AF1716423...

Douglas A. Swank, Member.

DocuSigned by:
Richard Van Emmerik
3EB0DB6FD00E416...

Richard Van Emmerik, Department Head
Department of Kinesiology

DEDICATION

I dedicate this work to my parents, for their continuous work and sacrifice in supporting myself and my two younger brothers.

ACKNOWLEDGEMENTS

I would like to thank my advisor and mentor, Mark Miller, Ph.D. for taking a chance with a Nutrition major who only knew how to bend T-clips. Your guidance and support over the last four years has allowed me to be in the position I am today. Thank you to the rest of my committee, Jane Kent, Ph.D., Edward Debold, Ph.D., and. Douglas Swank, Ph.D. for your help with this project.

I want to thank Jesse Mager, Ph.D. for graciously offering the mice used in this study.

I would like to thank all the members of the Muscle Biology Lab that I have interacted with over the last four years. Current members Brent Momb, Christopher Lee, Matthew Limoges – thank you for sitting through hours after hours of the same presentation and continuing to provide feedback. Prior members of Gregory Spicer, Ph.D., Shayelia Stanley, Anudeep Jala, Kim Unger, Caroline Pellegrini, Aurora Foster, Chad Straight, Ph.D. - you were all greatly influential during my time as a graduate student. Special thanks to Aurora Foster and Chad Straight, Ph.D. who were my lifeline when first joining the lab. I would not have pursued this career if I hadn't stumbled across you two. Thank you to the rest of the Kinesiology Department for keeping me on my toes, especially Brent Scott, Ph.D. for introducing me into the world of R coding.

I want to thank all my friends and family, especially my mom and dad. Your commitment and guidance during my upbringing allowed me to flourish into the man I am today. I love you both dearly.

ABSTRACT

STRETCH ACTIVATION DURING FATIGUE IMPROVES RELATIVE FORCE PRODUCTION IN FAST-CONTRACTING MOUSE SKELETAL MUSCLE FIBERS

FEBRUARY 2023

PHILIP C. WOODS, B.S., UNIVERSITY OF MASSACHUSETTS AMHERST

M.S., UNIVERSITY OF MASSACHUSETTS AMHERST

Directed by: Professor Mark S. Miller.

Stretch activation (F_{SA}) is the delayed increase in fiber specific tension (force per cross-sectional area) following a rapid stretch and can improve muscle performance during repetitive cyclical contractions. Historically considered minimal in skeletal muscle, our recent work showed the ratio of stretch- to calcium-activated specific tension (F_{SA}/F_0) increased from 10 to 40% with greater inorganic phosphate (Pi) levels in soleus muscle fibers (Straight et al., 2019). Given Pi increases with muscle fatigue, we hypothesize that F_{SA} helps maintain force generation during fatigue. To test this, F_{SA}, induced by a stretch of 0.5% fiber length, was examined during Active (pCa 4.5 (pCa = -log([Ca^{2+}]), pH 7.0, Pi 5 mM), High Ca^{2+} Fatigue (pCa 4.5, pH 6.2, Pi 30 mM) and Low Ca^{2+} Fatigue (pCa 5.1, pH 6.2, Pi 30 mM) in fibers expressing myosin heavy chain (MHC) I, IIA, IIX and IIB isoforms from soleus and extensor digitorum longus muscles of C57BL/6NJ mice. F_0 of all MHC isoforms decreased from Active to High Ca^{2+} Fatigue to Low Ca^{2+} Fatigue, as expected. In MHC IIX and IIB fibers, F_{SA} occurred under all conditions and F_{SA}/F_0 increased from Active (17-20%) to High Ca^{2+} Fatigue (32-35%) to Low Ca^{2+} Fatigue (42-44%). In MHC IIA fibers, F_{SA}/F_0 increased similarly

to MHC IIX and IIB fibers from Active (14%) to High Ca^{2+} Fatigue (32%) but stayed elevated under Low Ca^{2+} Fatigue (35%). For MHC I fibers, no discernable F_{SA} was apparent in either High – or Low Ca^{2+} Fatigue, leaving an F_{SA}/F_0 value in Active only (4%). These results show that F_{SA} is a significant modulator of specific tension production under fatiguing conditions in fast-contracting muscle fibers. This mechanism could play an important physiological role during cyclical contractions, when the antagonistic muscle rapidly stretches the agonist muscle, by reducing the effect of fatigue on specific tension production.

TABLE OF CONTENTS

Page

ACKNOWLEDGEMENTS iv

ABSTRACT v

LIST OF TABLES x

LIST OF FIGURES xi

GLOSSARY xii

CHAPTER

1. INTRODUCTION 1

1.1 Background 1

1.2 Study Approach 3

1.3 Aims and Hypothesis 3

2. LITERATURE REVIEW 5

2.1 Introduction 5

2.2 Stretch Activation 5

2.2.1 Overview 5

2.2.2 Insect Flight Morphology 7

2.2.3 Discovery of Stretch Activation 10

2.2.4 Cardiac Tissue 11

2.2.5 Skeletal Muscle 11

2.2.6 Shortening Deactivation 21

2.3 Proposed Mechanisms of Stretch Activation 23
2.3.1 Early Work 23
2.3.2 Current Supported Hypothesis 23
2.3.3 Potential Myosin-Based Mechanism 24
2.4 Skeletal Muscle Fatigue 26
2.4.1 Overview 26
2.4.2 Biochemical Changes *in-vivo* 27
2.4.3 Classifying fatigue into phases 28
2.5 Summary 32
3. METHODS 34
3.1 Introduction 34
3.2 Mice 34
3.3 Experimental Preparation 34
3.3.1. Location 34
3.3.2. Experimental Apparatus 35
3.3.3 Experimental Solutions 35
3.3.4. Muscle Tissue Processing 36
3.3.5. Preparation of Single Fibers 37
3.3.6 Single Fiber Mechanical Measurements 37
3.3.7 Myosin Heavy Chain Isoform Composition 40
3.4 Analysis of Stretch Activation 40

3.5 Statistics 41

3.6 Proof of Concept 41

4. RESULTS 44

4.1 Introduction 44

4.2 Single Fiber Mechanical Measurements 46

5. DISCUSSION 51

5.1 Introduction 51

5.2 Physiological Relevance 53

5.3 Stretch Activation is lost in Slower-Contracting isoforms 54

5.4 Comparison of Aims 55

5.4 Molecular Mechanism 60

5.5 Limitations and Future Directions 62

BIBLIOGRAPHY 64

LIST OF TABLES

Table Page

1. Single Fiber Mechanical Measurements……45

2. Summary of Fatigue's Effects on Stretch Activation……52

3. Solution Constituents Differences Between Studies……..59

4. Fiber Identification Differences Between Studies…….59

LIST OF FIGURES

Figure Page

1. Depiction of Stretch Activation……...6

2. Stretch Activated Response Across Striated Muscle……...7

3. EMG vs. Wing position in Insects……...9

4. Kinetics of Stretch Activation vs. Unloaded Shortening ……..…14

5. Kinetics of Stretch Activation within MHC isoforms……...16

6. Influence of Pi on Stretch Activation within *Drosophila*……..18

7. Stretch Activation vs. Pi within Mammalian Skeletal Muscle……..……....20

8. Depiction of Shortening Deactivation……...22

9. Myosin-based Mechanism of Stretch Activation……...26

10. Pi and pH Changes During Muscle Fatigue……..…….28

11. Declines in Intracellular Calcium During Fatigue…….30

12. Summary of Muscle Fatigue……..32

13. Sinusoidal Analysis Rig…….38

14. Preliminary Data……43

15. Results: Calcium-activated Specific Tension……46

16. Results: Stretch-activated Specific Tension……...47

17. Results: Stretch-to-Calcium-activated Specific Tension……...48

18. Results: Rate of Stretch Activation……49

19. Results: Average Force Trace for each MHC isoform……..……...50

20. Model of Human Locomotion……...53

21. Rate of Force Development under Fatigue……55

GLOSSARY

- SA; Stretch Activation
- Specific Tension; Force Normalized to Cross-Sectional Area, mN/mm^2
- CSA; Cross-Sectional Area
- Ca^{2+}; Calcium
- $[Ca^{2+}]$; Calcium Concentration
- F_{SA}; Magnitude of Stretch Activated Specific Tension
- F_0; Calcium Activated Isometric Specific Tension
- DVM; Dorsal Ventral Muscle
- DLM; Dorsal Longitudinal Muscle
- IFM; Indirect Flight Muscles of Insects. Composed of the DVM and DLM
- Pi; Inorganic Phosphate
- *Drosophila Melanogaster;* Fruit Fly Insects
- [Pi]; Inorganic Phosphate Concentration
- EMB; Embryonic Isoform of Myosin
- IFI; Indirect Flight Isoform of Myosin
- pCa; $-\log([Ca^{2+}]$
- H^+; Hydrogen Protons
- ATP; Adenosine Triphosphate
- ADP; Adenosine Diphosphate
- CK; Creatine Kinase
- Pcr; Phosphocreatine
- Ryr; Ryanodine Receptors

- Initial Phase of Muscular Fatigue; Ph = 6.2, [Pi] = 30 Mm
- Secondary Phase of Muscular Fatigue; Ph = 6.2, [Pi] = 30 Mm, pCa 5.1
- EDL; Extensor Digitorum Longus
- BES; N,N-Bis[2-Hydroxyethyl]-2-Aminoethanesulfonic Acid
- EGTA; Ethylene Glycol-Bis(2-Aminoethylether)-*N*,*N*,*N*, *N*-Tetraacetic Acid
- Mg^{2+}; Magnesium
- DTT; Dithiothreitol
- CPK; Creatine Phosphokinase
- ML; Muscle Length
- Phase 1; Immediate Specific Tension Increase
- Phase 2; Rapid Specific Tension Decay
- Phase 3; Delayed, Secondary Specific Tension Increase. Magnitude Of Phase 3 is F_{SA}
- Phase 4; Slow Specific Tension Decay
- T_3; Measured from the Initiation of the Rapid Fiber Length Change to the Point in Time of the Greatest F_{SA} Value (Time of Phase 1 to Phase 3). Often Signified as Rate (r_3)
- Tnt; Tropomyosin-Binding Troponin
- V_{max}; Maximum Unloaded Shortening Velocity
- Matpase; Myofibrillar Adenosine Triphosphatase
- MHC; Myosin Heavy Chain
- Jump Muscle; Tergal Depressor of The Trochanter. Muscle That Powers Jump Prior To Flight in *Drosophila Melanogaster* Insects

- SD; Shortening Deactivation
- F_{SD}; Magnitude of Stretch Deactivated Specific Tension
- Rate Of SD; Rate of Shortening Deactivation
- SDS-PAGE; Sodium Dodecyl Sulfate-Polyacrylamide Gel Electrophoresis
- $2\pi b;$ The Rate of Myosin Transition from Weakly To Strongly Bound State

CHAPTER 1

INTRODUCTION

1.1 Background

Stretch activation (SA), or the delayed increase in specific tension (force normalized to cross-sectional area (CSA), mN/mm^2) following a rapid stretch of a calcium (Ca^{2+}) activated muscle fiber (57, 65, 72, 76, 77), is a mechanical phenomenon that is a general property of all muscle (57). Originally discovered in the late 1940's within insects (64), ample evidence has emerged highlighting the magnitude of SA (often signified as F_{SA}) and the vital role this delayed specific tension has within insect locomotion. Insect flight requires high frequency contractions of their indirect flight muscles (IFM), particularly the Dorsal Ventral (DVM) and Dorsal Longitudinal (DLM) muscles. To maintain the work required at these higher frequencies, insects evolved to adapt SA within the DVM and DLM as their primary mode of power production (77). By the 1970's, SA was observed within cardiac tissue (71) with evidence suggesting F_{SA} aids with cardiac output (11, 71–73). Within the same decade SA was observed within skeletal muscle (68, 72), however unlike IFM and cardiac tissue skeletal muscle seemed to have no apparent physiological use for this phenomenon. Due to skeletal muscles high production of Ca^{2+} activated specific tension (F_0) and low F_{SA}, minimal investigative efforts of SA were put forth into this tissue.

Recently, promising data has emerged suggesting that F_{SA} is partially influenced by inorganic phosphate (Pi) in slow-contracting skeletal muscle fibers. Within *Drosophila melanogaster* (fruit fly), modifications of the jump muscle to express a slow-

contracting embryonic isoform (EMB) saw F_{SA} increase in the presence of moderate concentrations of Pi ([Pi]) (90), while expression of a fast-contracting indirect flight isoform (IFI) saw no change in F_{SA} with similar [Pi] (91). Furthermore, in single muscle fibers from the slow-contracting soleus and the fast-contracting extensor digitorum longus (EDL) of female mice, F_{SA} increased in soleus muscle fibers but decreased in EDL fibers as Pi increased from low to moderate concentrations (76). Together these findings suggest that in the presence of Pi, SA seems to improve specific tension in skeletal muscle fibers of slow-contracting muscles.

Physiologically, this could help to modulate specific tension production in slow-contracting fibers during fatigue. Skeletal muscle fatigue is defined as the decreased ability for muscles to generate force or power due to a reduction in contractile velocity and/or specific tension in response to contractile activity (46, 47). During extended muscle activity Pi accumulation occurs, which has been shown to inhibit skeletal muscle's ability to produce F_0 (47). However, while prolonged skeletal muscle utilization does contribute to increases in Pi, Pi is not the only metabolic by-product that accumulates during these conditions. Hydrogen ions (H^+), measured by a drop in intracellular pH, also begin to accumulate within the myoplasm during fatigue (9). Declines in intracellular pH have also been shown to inhibit the cross-bridge cycle, leading to a decline in F_0 (4, 16, 23). Additionally, accumulation of both Pi and H^+ have been shown to disrupt Ca^{2+} sensitivity of single muscle fibers (16, 17, 23, 58), and may impact Ca^{2+}concentration [Ca^{2+}] of the myoplasm by reducing Ca^{2+} release from the sarcoplasmic reticulum (17, 83). Together, disruptions of Ca^{2+} sensitivity and/or [Ca^{2+}] further diminish single muscle fibers' ability to produce F_0. Whether F_{SA} demonstrates a

similar response of modulating specific tension in slow-contracting skeletal muscle fibers, as observed with increases in F_{SA} in the presence of Pi, within conditions that are more representative of *in vivo* physiology are unknown. Particularly, investigation of the response of F_{SA} in conditions of elevated Pi and H^+ and decreased $[Ca^{2+}]$ in single skeletal muscle fibers are warranted.

1.2 Study Approach

The objectives of this study were to: 1) Determine SA's response during simulated conditions of the initial, metabolite induced phase of muscular fatigue (30 mM Pi, pH 6.2) and 2) compare the contribution of SA to total specific tension during the initial vs secondary, Ca^{2+} induced (30 mM Pi, pH 6.2, pCa 5.1 ($pCa = -\log([Ca^{2+}])$) phases of muscular fatigue in soleus and EDL muscle fibers. Single muscle fibers were collected from both the soleus (slow contracting) and EDL (fast contracting) muscles from female mice and were exposed to four experimental conditions. Fiber specific tension and single fiber mechanical measurements were performed in each experimental condition.

1.3 Aims and Hypothesis

Aim 1: Quantify F_{SA} during the initial, metabolite induced (Pi = 30 mM, pH = 6.2) stage of muscular fatigue in mouse soleus and EDL skeletal muscle fibers.

Hypothesis for Aim 1: F_{SA} will increase during the metabolic induced stage of fatigue in soleus (slow contracting) and decrease in EDL (fast contracting) skeletal muscle fibers compared to non-fatiguing conditions.

Aim 2: Quantify F_{SA} during the secondary, Ca^{2+} induced (30 mM Pi, pH 6.2, pCa 5.1) stage of muscular fatigue and compare SA's potential role in modulating specific tension production between initial and secondary phases of muscular fatigue.

Hypothesis for Aim 2:F_{SA} will decrease in lower [Ca^{2+}] (secondary) fatigue conditions compared to the higher [Ca^{2+}] (initial) fatigue conditions for both soleus (slow contracting) and EDL (fast contracting) muscle fibers, with soleus fibers' F_{SA} being greater compared to EDL fibers' F_{SA} in lower [Ca^{2+}] (secondary) fatigue conditions.

CHAPTER 2

LITERATURE REVIEW

2.1 Introduction

This literature review will first provide an overview of SA, including the discovery of SA with insect flight morphology. SA within various types of striated muscle will follow, with a focus on skeletal muscle. Next, the supported underlying mechanism for SA in IFM and cardiac muscle will be examined, as well as a recently proposed mechanism within skeletal muscle. Lastly, as this project proposes to examine the effects of SA during fatigue, *in vivo* metabolic changes during skeletal muscle fatigue will briefly be discussed.

2.2 Stretch Activation

2.2.1 Overview

As depicted in **Figure 1**, following a rapid length increase (0.5% of muscle length (ML)) of a Ca^{2+} activated muscle, the specific tension transient displays a four-phase response: an immediate increase (Phase 1), a rapid decay (Phase 2), a delayed and slower secondary increase (Phase 3), and a delayed and slower secondary decay (Phase 4) (24). F_{SA} is the greatest magnitude of specific tension that occurs during Phase 3. The timing of this peak (often signified as t_3, seconds or r_3, s^{-1}) is measured from the initiation of the rapid fiber length change to the point in time of the greatest F_{SA} value. While the name may suggest muscle activates by stretch alone, stretching relaxed tissue shows no sign of enhanced activation and simply behaves like a passive viscoelastic material (57).

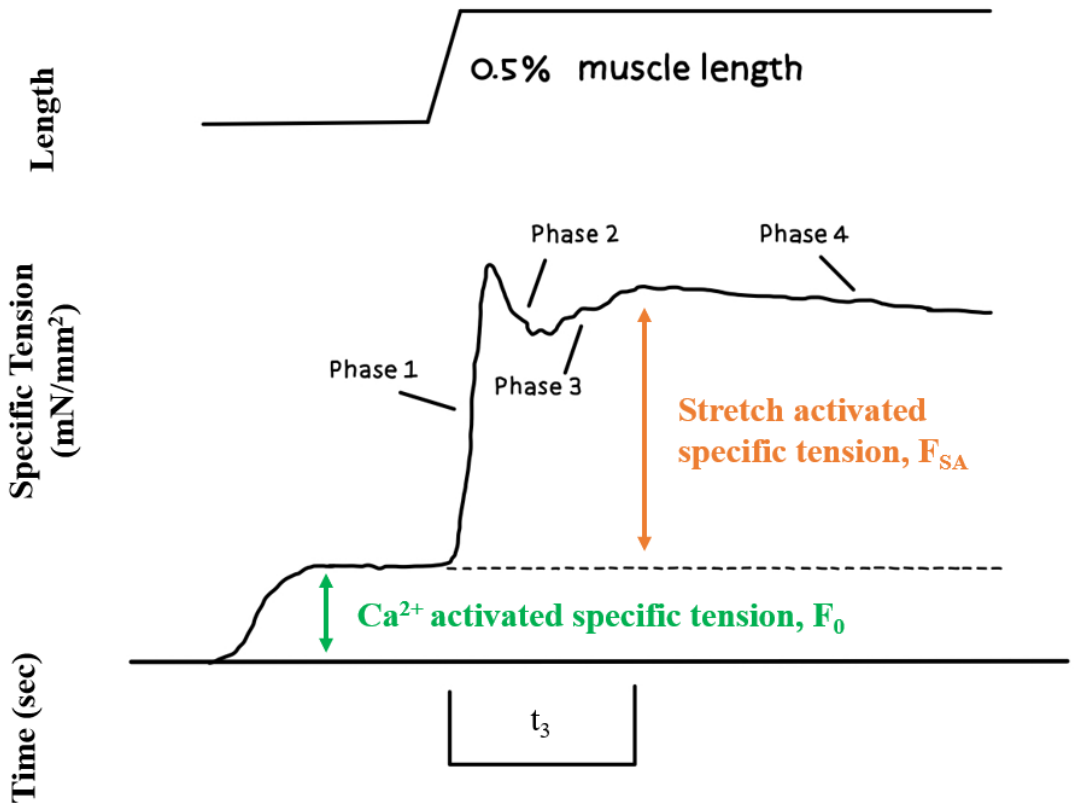

Figure 1: SA caused by an increase in ML. Length (top), specific tension (middle), and time (bottom) traces from a *Drosophila melanogaster* (fruit fly) IFM undergoing a 0.5% ML increase. The four phases of the tension response are indicated along with F_0 and F_{SA}. F_{SA} is typically 2-3-fold higher than F_0 in fruit fly IFM. Figure modified from (77).

Both F_{SA} and t_3 dictate SA's physiological relevance. *In vivo* antagonistic muscle pairs that undergo oscillatory contractions, in which a contraction of the antagonist muscle stretches the agonist muscle, benefits from this mechanical response when the delayed increase in specific tension happens to coincide with the agonist muscle shortening. This either contributes or enables muscles to produce positive work depending on the muscle type (77). While SA is a general property of all muscle (40, 41, 57, 65, 71, 72), historically this response has been investigated within three cases of striated muscle: IFM of insects as well as cardiac tissue and skeletal muscle of mammals. **Figure 2** demonstrates the stark difference in F_{SA} patterns (Phase 3) between different

striated muscle types. IFM, which produces very small F_0, depends highly upon its large F_{SA} to power wing contractions during flight. Cardiac tissue incorporates both moderate F_0 and F_{SA} for the process of ejecting blood from the heart and throughout the circulatory system. Skeletal muscle produces large F_0 but low F_{SA}, and as such this phenomenon has often been considered physiologically irrelevant in this tissue.

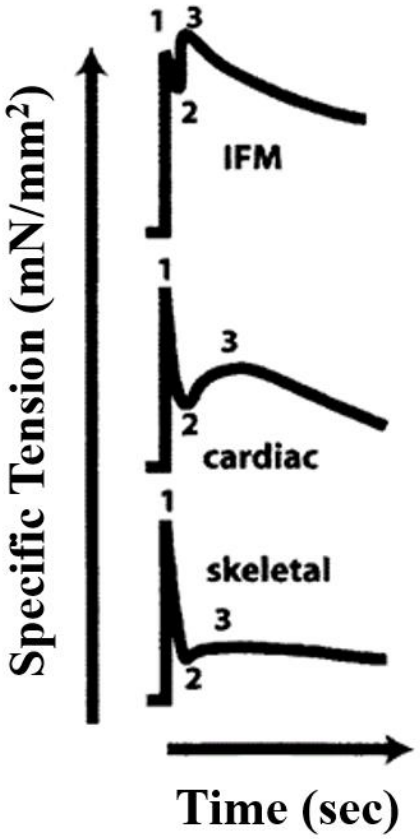

Figure 2: The amplitude of the stretch activation (3) response across striated muscle. Figure modified from (57).

2.2.2 Insect Flight Morphology

There are two distinct muscular systems that insects have developed evolutionarily to help achieve flight, known as direct/synchronous and indirect/asynchronous muscles (7). As the name implies, contractions of direct flight

muscles directly raises and lowers the wings (57, 64), while contractions of IFM cause a deformation of the thoracic cuticle, ultimately leading to wing movement (77). Direct flight muscles are often referred to as synchronous due to the 1:1 relationship between motor unit action potential and muscle contractions, while IFM often demonstrate no strict correlation between electrical and mechanical events and as such are referred as asynchronous (42). **Figure 3** provides a demonstration of both the neural activity and resulting wing motion of the *Schistocerca americana* locust (synchronous – bottom trace), where an EMG spike occurs at the start of each cycle of the wing position, and the *Cotinus mutabilis* beetle (asynchronous – top trace) where one EMG spike causes multiple cycles of the wing position to occur.

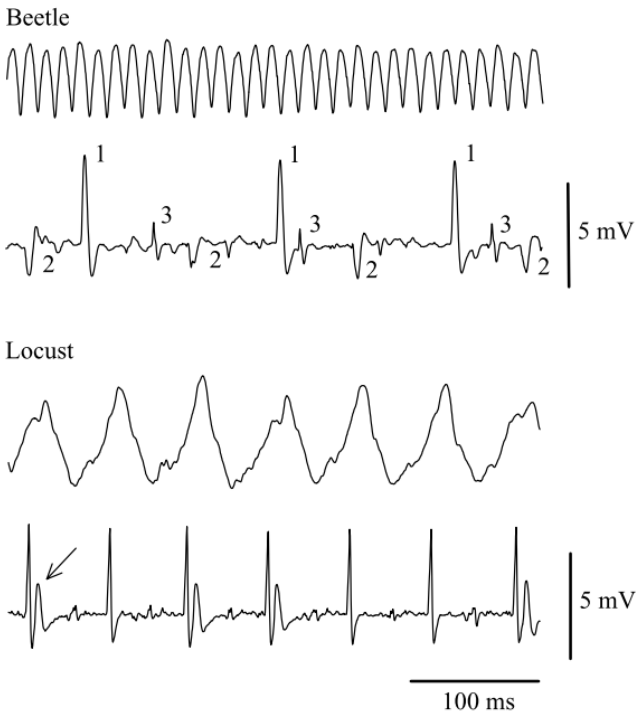

Figure 3: Wing position (top trace in each Beetle and Locust data) and muscle action potentials (electromyogram recordings, EMGs) during tethered flight. Action potentials from three motor units are evident in the beetle EMG trace. These units are labeled 1–3 in order of decreasing size. Each wing stroke of the locust muscle is associated with an action potential or a pair of action potentials (an example of a second action potential is marked with an arrow). Figure from (42).

During insect flight, many insects beat their wings at an extremely rapid rate, ranging anywhere from 100 to 1000 Hz (57). The direct/synchronous muscular system can work at these higher frequencies in part due to the development of an extensive sarcoplasmic reticulum and narrow myofibril, which allows rapid Ca^{2+} release and reuptake. However unlike the direct/synchronous system, the sarcoplasmic reticulum is a minimal component of the indirect/asynchronous system (42), and along with very large myofibrils (57) the metabolic cost for pumping Ca^{2+} in and out of the sarcoplasmic reticulum at higher frequencies is too great for insects containing the indirect/asynchronous system (42). Instead of cycling Ca^{2+} into the myoplasm for each

contraction, the indirect/asynchronous system of *Drosophila* and other insects relies primarily on SA for specific tension production during flight (33). Indirect/asynchronous cyclical contractions operate first via a primed level of stimulation provided by a fixed [Ca^{2+}] which initiates contraction of the DVM and DLM, the antagonist muscle pair that raises and lowers the wings, respectively (10). Once primed, the contraction of one of these dorsal muscles will cause the other to stretch, generating F_{SA}. Repeated cyclical contractions generate F_{SA} for both the DVM and DLM, which is then used to power both muscles for continuous flight. Asynchronous muscles are only believed to occur in insects, with an estimated three-quarters of all insect species using asynchronous flight muscles (19, 42). Overall, direct/synchronous insect flight muscles contract similarly to mammalian skeletal muscle where [Ca^{2+}] changes with each contraction that is initiated by electrical stimulation, while indirect/asynchronous flight muscle have a constant [Ca^{2+}] and rely upon SA to produce oscillatory motion.

2.2.3 Discovery of Stretch Activation

SA was first discovered within indirect flight muscles of *Calliphora* (blow fly) insects (64). During the mid-20th century researchers were interested in understanding indirect flight muscle physiology, specifically the DVM and DLM, since these muscles differed considerably in their appearance compared to other insect muscles. Using *Calliphora* flight muscles, Pringle (64) observed a disconnect between the action potentials for indirect flight muscles and wing movement, where multiple wing thrusts were observed with only a few electrical stimuli (similar to findings of that in **Figure 3**). Traditional skeletal muscle contractions require an individual electrical stimulus for each muscle twitch, and this observation within the *Calliphora* insects led Pringle to

hypothesize that the electrical stimulus seemed to prepare the contractile elements to respond to the stretch of the antagonist muscle, with the repetition of this process leading to oscillatory excitation of the DLM and DVM (64). Similar findings were reproduced (67) in several flies and a wasp, however cockroaches and moths demonstrated a 1:1 relationship between action potential and wing thrust, noting insect flight muscle physiology via stretch is not universal between species.

2.2.4 Cardiac Tissue

SA within cardiac tissue was observed in papillary and trabecular muscles of rabbits and guinea pigs (71), and the first hint of physiological relevance was due to the kinetics of SA, specifically t_3 matching to mammalian heart rates (71–73). SA is widely considered to play a role in aiding myocardial power generation and systolic ejection (74). The rhythmic pattern that cardiac muscle displays is analogous to the rhythmic contractions observed in the IFM (11) and while the underlying mechanism is still undetermined, SA within cardiac tissue is hypothesized to be of similar nature to that found within IFM (see **2.3 Proposed Mechanisms of Stretch Activation**).

2.2.5 Skeletal Muscle

Overview. SA was initially believed to be confined solely to IFM until the 1970s, two decades after its first discovery, when a sizeable body of evidence indicated SA was a common property of all muscular tissue (72). Investigation into SA within skeletal muscle has received the least attention, in part due to the delayed tension response having the smallest amplitude compared to IFM and cardiac tissue (**Figure 2**) (57), which has led to the assumption that this phenomenon is of limited importance within this tissue.

Specific investigation of the mechanism within skeletal muscle began with abrupt stretches on rabbit psoas and frog semitendinosus muscle bundles in varying temperatures and [Ca^{2+}] (68). A similar biphasic response, with an immediate rise and fall of specific tension followed by another delayed tension rise was observed in both rabbit psoas and frog semitendinosus muscle bundles. However specific tension responses to stretching were slower for the frog's semitendinosus, foreshadowing SA's variability between muscle groups. Furthermore, timing of SA was highly dependent on temperature, as t_3 shortened as temperatures increased (68). Other early investigations implementing muscle length alterations for understanding skeletal muscle mechanisms, without directly investigating SA, observed similar patterns of delayed specific tension changes in response to lengthening in a variety of tissues including the cicada tymbal muscle (1), frog sartorius (38), tortoise ileofibularis muscle (37), frog anterior tibial muscle (44), and crayfish fibers (45). SA kinetics within different muscle types was examined and compared to maximum unloaded shortening velocity during the 1990s (28–31). More recently, F_{SA} within skeletal muscle has received more attention, with work initially conducted in the tergal depressor of the trochanter of insects (90, 91) and then with lower extremity muscles of female mice (76).

Kinetics of Stretch Activation and Fiber Typing. Throughout the last decade of the 20th century a research group from Germany began to explore the relationship between skeletal muscle SA kinetics and fiber types. Led by researcher Dr. Stefan Galler, their first publication compared t_3 and maximum unloaded shortening velocity (V_{max}) to fiber types in rat, fish, crayfish and locust skeletal muscle fibers (28). Their goal was to determine whether a correlation existed between fiber types and the timing of SA, as

prior investigators had difficulties building strong correlations with V_{max} and fast fiber types (8). Fiber type identification were histochemically defined via their myofibrillar adenosine triphosphatase (mATPase) activity, a staining methodology that evaluates fiber types based on pH sensitivity (21, 70). T_3 was found to be longer in the slower fiber types and shorter in the faster independent of species (28). Furthermore, t_3 values were always significantly different within varying fiber types for each species, while V_{max} values overlapped for intermediate and higher mATPase active fibers. The authors concluded that t_3 had a stronger correlation with fiber types than V_{max}, however no correlation coefficients were provided. Regardless, this study was the first to include an investigation of t_3 within different fiber types from varying organisms, highlighting the newly discovered relationship fiber types had on SA kinetics within skeletal muscle.

While ATPase activity is a common classification scheme used in the literature to experimentally define fiber types, the methodology's ability to accurately identify the subdivisions of the fast fiber types is a large limitation (66). Myosin heavy chain (MHC) identification is another common methodology used for fiber type classification, which measures the composition of the heavy meromyosins within a muscle fiber (70). This classification system can distinguish between hybrids of the faster isoforms more accurately than ATPase, and overall serves as a less subjective method (66). Considering the findings with ATPase activity and t_3, Galler and colleagues focused their investigations on stretch activated kinetics and MHC isoforms, first replicating the comparison to V_{max} values (30), then to tropomyosin-binding troponin subunits (27), and lastly comparing t_3 between species (29).

Using skeletal muscle fibers from a male rat, Galler and colleagues noticed a similar relationship with t_3 and MHC composition to that previously reported with ATPase activity (28). T_3 values had clear distinctions between MHC isoforms (**Figure 4-A**). The authors claimed neighboring MHC isoforms were "statistically different from one another" (30), however that statement is severely limited by the use of significance being $P < 0.1$ and hybrid isoforms seemingly overlapping one another. V_{max} values did demonstrate larger variability between MHC isoforms, with most MHC II values overlapping (**Figure 4-B**). Once again, the authors stated that t_3 had a stronger correlation with MHC than V_{max}, however no correlation coefficients were provided. What is apparent is that the variability with t_3 values seems to be less compared to V_{max}, as demonstrated by the error bars in **Figure 4**. Both findings of less variability with t_3 and fiber types, including both ATPase identification (28) and MHC isoforms (30) cemented the understanding that SA kinetics are influenced by fiber types.

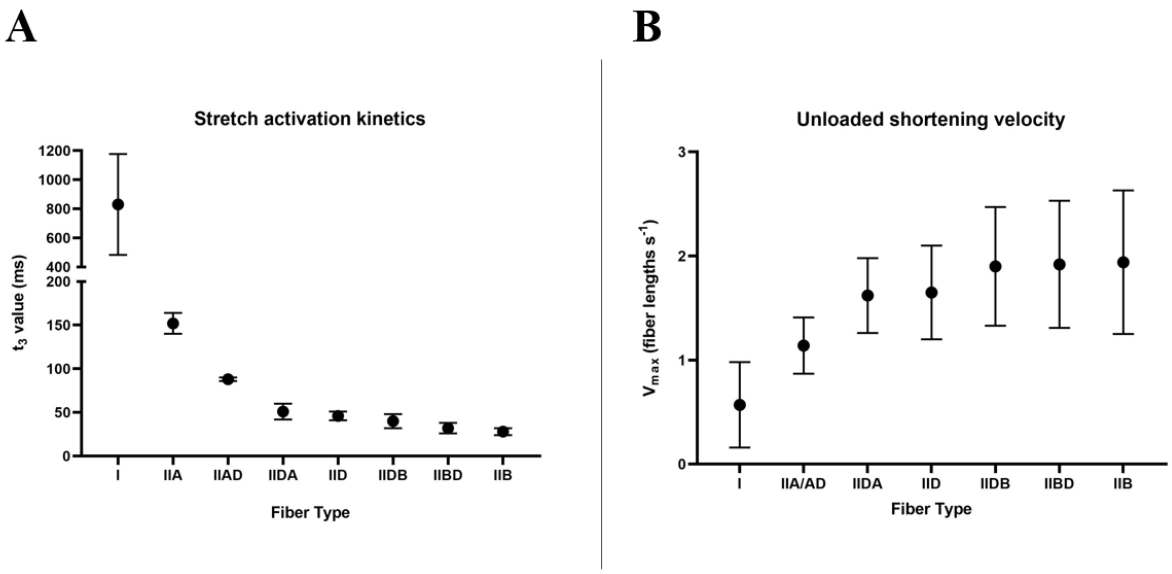

Figure 4: Kinetic parameters of (**A)** stretch activation and (**B**) unloaded shortening velocities on single skinned-fiber preparations from an adult male Wistar rat. Muscle fibers were collected from the tibialis anterior, gracilis, adductor magnus, vastus lateralis and soleus. Figure of Table 1 from (30).

However, one potential problem with this interpretation is that isoforms of other myofibrillar proteins besides the heavy meromyosin can be coexpressed with MHC isoforms and potentially weaken this relationship (27). Characterized by both MHC isoform and tropomyosin-binding troponin (TnT) subunit isoforms was a procedure taken to examine the possible influence other myofibrillar proteins could have on t_3. TnT is the most likely candidate for another myofibrillar protein having influence beyond myosin due to a multitude of reasons, primarily being that TnT has the second highest molecular diversity behind MHC (63). Two slower isoforms (TnT_{1s}, TnT_{2s}) and four faster isoforms (TnT_{1f}, TnT_{2f}, TnT_{3f}, TnT_{4f}) were identified from muscle fibers of an adult male rat. Examination showed no correlation between the t_3 and any of the TnT_f isoforms, as fibers that did not display TnT_f still had a strong relationship between MHC and t_3 (27). Data from this study were unable to rule out the possible influence TnT_s isoform had on t_3, however it is unlikely that other myofibrillar proteins are responsible for the range in kinetics. Overall, this further corroborates the relationship between SA kinetics and MHC isoforms.

When comparing the relationship between MHC isoform and SA kinetics across various species, t_3 was different between pure MHC I, IIA, IID, and IIB isoforms, as expected from previous work (30). Interestingly, MHC I and IIA showed similar t_3 values between the three species examined (rat, rabbit, and human) (**Figure 5**). This evidence of similar SA kinetics in the same MHC isoform across species is interesting since MHC isoform kinetics (36) and ATPase activity (6) are not homogeneous between different mammalian species.

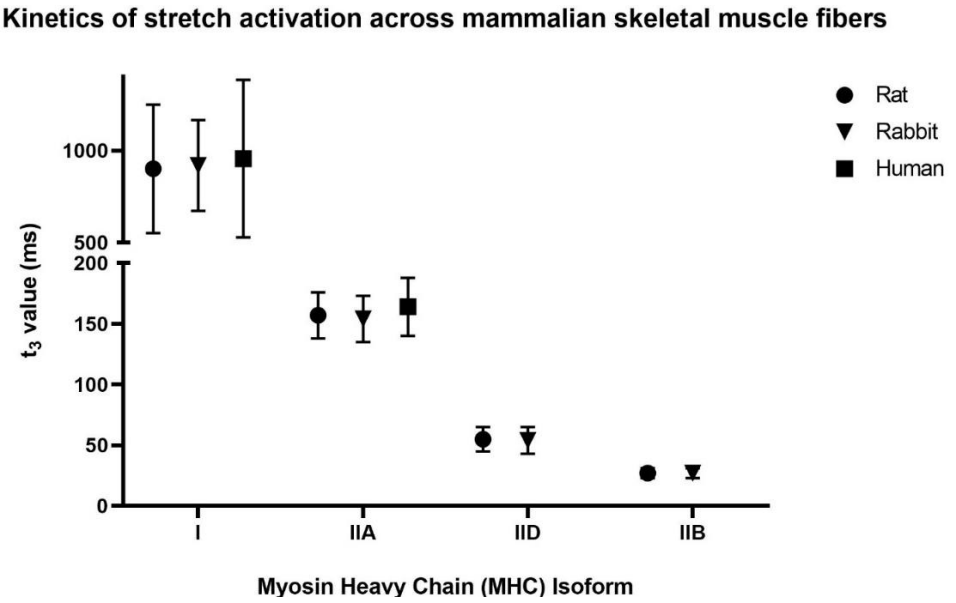

Figure 5: Kinetics of stretch activation, expressed by the t_3 value in rat, rabbit, and human muscle fiber types at 22-24°C. Muscle fibers originated from the soleus, tibialis anterior, extensor digitorum longus, psoas, gastrocnemius, gracilis, vastus lateralis and adductor magnus muscles of the Sprague Dawley rat and from the adductor magnus and soleus muscles of a White New Zealand rabbit. Human muscle fibers from the rectus femoris were taken from one of the authors (S.G.) and only displayed MHC I & IIA isoforms. Figure of Table 1 from (29).

*Specific Tension of Stretch Activation (F_{SA}) and Inorganic Phosphate (Pi).*The tergal depressor of the trochanter (TDT), or more commonly known as the jump muscle, is the second commonly used thoracic muscle from *Drosophila* in muscle investigation besides the IFM due to both muscles straightforward ability to undergo gene mutation (77, 80). As the name implies, this muscle powers the act of jumping, which for *Drosophila* typically happens immediately before flight. Structurally different than IFM, the jump muscle is thought to be synchronous and behaves more similar to skeletal muscle with activation due to intracellular Ca^{2+} rather than SA (61, 77).

In hopes of developing an understanding of the molecular basis of SA, Zhao & Swank developed two experimental conditions in which they genetically modified the

MHC isoform of the jump muscle. One modification was made to express a slow-contracting EMB isoform (90) and the other with the fast-contracting IFI (91). For each genetic modification, F_{SA} was compared at 0-, 8-, and 16 mM Pi. Expression of the slower EMB isoform decreased r3 at both 8- and 16-mM Pi compared to control (**Figure 6A**), which is the same as saying t_3 increased with the expression of the slower EMB isoform, as the rate of Phase 3 is $1/t_3$. This finding of altered Phase 3 timings with changes in MHC expression is unsurprising with MHC isoform's influence on kinetics as previously described (27–30), however what was surprising was the change in F_{SA}. In its natural isoform the jump muscle displays little F_{SA} (**Figure 6B-control**). However, when modified to express the slower EMB isoform the jump muscle experienced an 2.6-fold increase in F_{SA} at 8 and 16 mM Pi compared to 0 mM Pi (**Figure 6B-EMB**), allowing the fiber to produce positive work and power (90). Expression of the faster IFM isoform saw no change in F_{SA} at either 8 or 16 mM Pi compared to 0 mM Pi (**Figure 6C**) (91). F_{SA} was 1.7-fold higher for the IFM isoform compared to the native isoform (control) at 16 mM Pi, however that was the result of F_{SA} declining in the native isoform and staying unchanged in the IFM isoform at higher [Pi] (**Figure 6C**). These findings suggest two conclusions: 1) F_{SA} can be influenced by phosphate, as seen with the 2.6-fold increase at 8 and 16 mM Pi for the EMB expressing jump muscle (90) and, 2) $F_{SA,}$ along with t_3 seems to fiber-type specific, as F_{SA} seem to respond in slower isoforms (EMB) (90) but stay relatively unchanged for the fast isoform (IFM) (91) in the presence of Pi.

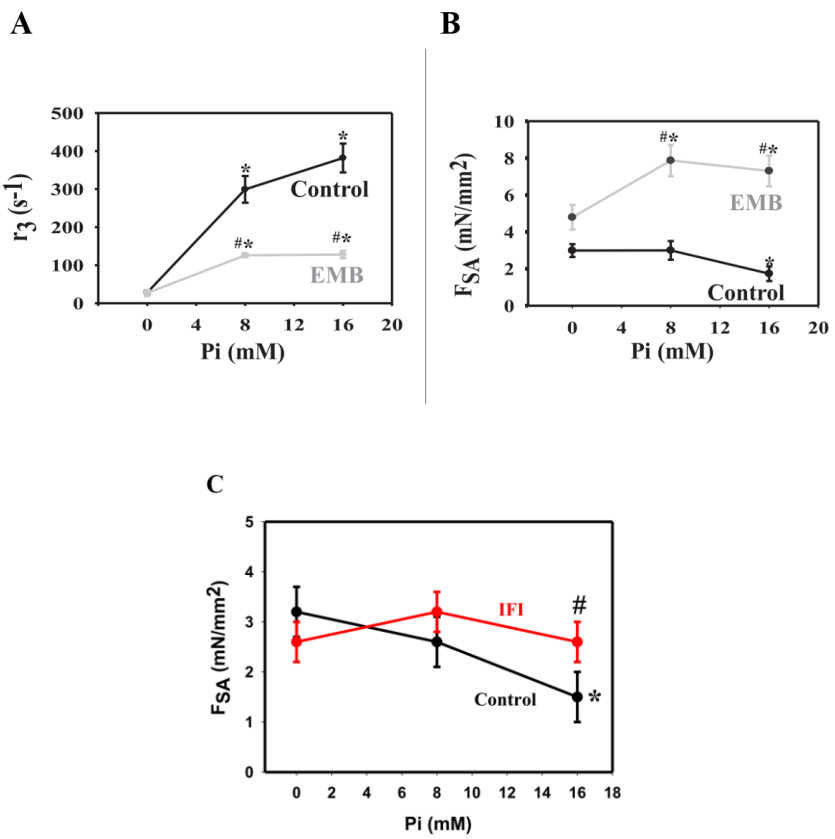

Figure 6: Influence of inorganic phosphate (Pi) on (A) rate of stretch activated specific tension regeneration, r3 and stretch activation specific tension (F_{SA}) of (B) EMB fibers (90) and (C)indirect flight isoform fibers (red) (91) compared to control jump muscle fibers (black). For (C), #P <0.05 compared with control and *P < 0.05 compared with 0 mM Pi.

One of the key features of the last two articles that allowed researchers to notice differences in F_{SA} between two distinct isoform expressions of the jump muscle was the presence of Pi. This outcome suggests that slower isoforms may benefit from SA during the presence of Pi. To experimentally investigate this hypothesis within skeletal muscle, Straight and colleagues compared F_{SA} values in varying [Pi] in soleus and EDL skeletal muscle fibers from female mice (76). F_0 and F_{SA} values were measured in [Pi] ranging from 2 – 16 mM. As expected, fibers from both muscle groups demonstrated similar losses to F_0 as [Pi] increased (see **Figure 7B**). However, fibers from the two muscles

responded differently to stretch, as F_{SA} declined in EDL but increased in soleus muscle fibers as [Pi] increased (**Figure 7A**). F_{SA}/F_0, or stretch activated specific tension divided by calcium activated isometric tension, is a ratio that normalizes F_{SA} to F_0 and allows for comparison of the amount of F_{SA} generated to the total F_0 generated at any given [Pi]. For the faster contracting EDL muscle fibers, since both F_0 and F_{SA} decreased, F_{SA}/F_0 stayed relatively unchanged, ranging from 15% at 0 mM to 19% at 16 mM Pi. Soleus muscle fibers on the other hand experienced a 30% increase in F_{SA}/F_0, going from 10% at 0 mM to 40% at 16 mM (**Figure 7C**).

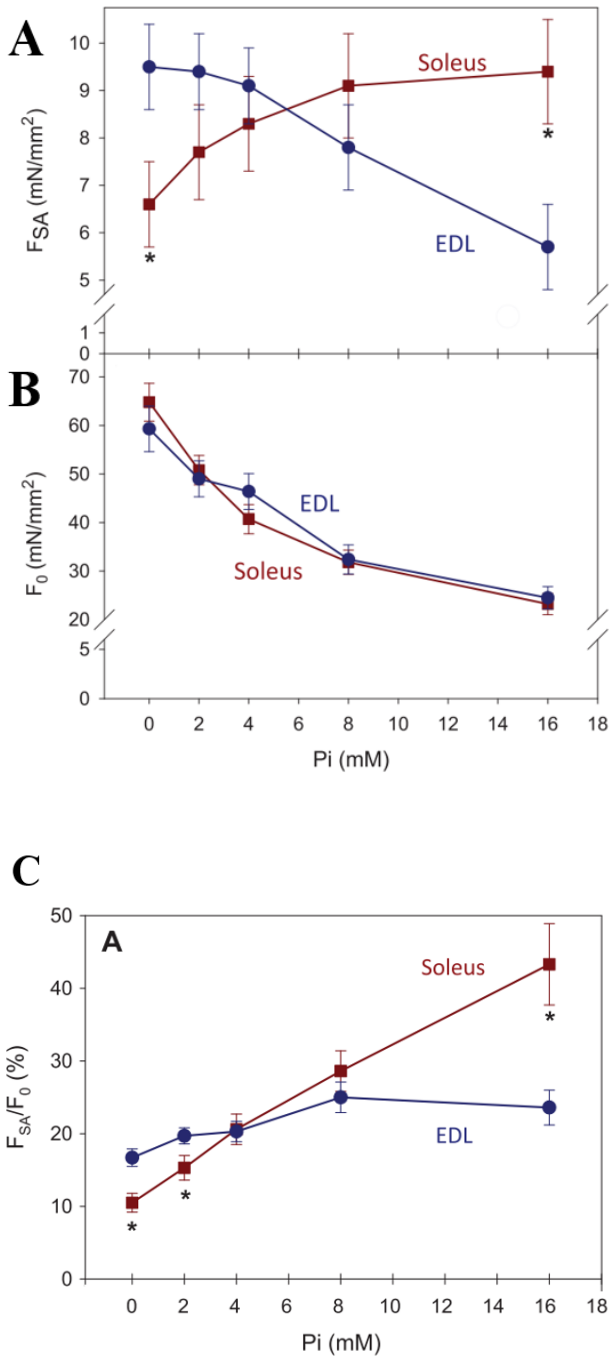

Figure 7: A: stretch activated specific tension, F_{SA}, increased for the slow-contracting soleus fibers, but decreased for the fast-contracting extensor digitorum longus (EDL) fibers with increasing Pi concentration ([Pi]). B: calcium activated isometric specific tension, F_0, decreased with increasing [Pi] for both soleus and EDL fibers. C: stretch activated specific tension, F_{SA}, normalized to calcium activated isometric specific tension, F_0. All values are means ± SE; n = 17 soleus fibers; n = 19 EDL fibers. *P < 0.05 compared with EDL at the same [Pi]. Figure from (76).

Clearly, soleus and EDL muscle fibers demonstrate opposite trends in response to [Pi], which is quite interesting considering Pi's known ability to inhibit specific tension generation. The authors conclude by stating the opposite trends observed provide evidence for "…a physiological reason for stretch activation in skeletal muscle fibers..." (76) suggesting SA may be relevant during muscular fatigue within certain muscle fibers, as Pi is a metabolic by-product of myosin-actin interactions and increases during muscular fatigue. However, there are limitations with this investigation that need to be addressed. Experiments were conducted at 17°C, which is not representative of *in-vivo* temperatures. The solutions used were designed for *Drosophila* physiology so results could be compared to Zhao and Swank's findings (90, 91), however using solutions designed for mammalian physiology could have an unknown influence on SA. Lastly, muscle fibers were identified solely based on their origin (i.e., soleus or EDL muscle) and lacked any fiber type classification (ATPase or MHC staining). Mouse soleus muscle is primarily composed of MHC I (37.42 ± 8.20%) and MHC IIA (38.62 ± 6.81%) isoforms while the EDL muscle is predominately MHC IIDB (21.48 ± 7.33%) and MHC IIB (66.01 ± 8.51%) (5). Whether the observed increase in F_{SA} at higher [Pi] is being driven by MHC I, IIA, or both is unclear. Future research addressing these issues, as well as incorporating major components of muscular fatigue, is warranted to determine if there is a physiological relevance for SA within skeletal muscle.

2.2.6 Shortening Deactivation

The opposite phenomenon to SA is shortening deactivation (SD), a delayed decrease in specific tension following muscle shortening (43, 51). When an Ca^{2+} activated muscle is shortened rapidly there will follow a similar but inverse four-phase

transient response (**Figure 8**). Similarly, the amplitude (F_{SD}) and timing (SD rate) of SD are measured. Physiologically this response may improve muscle relaxation, allowing the agonist muscle to relax quickly enough to not impede specific tension production for the antagonist muscle (51).

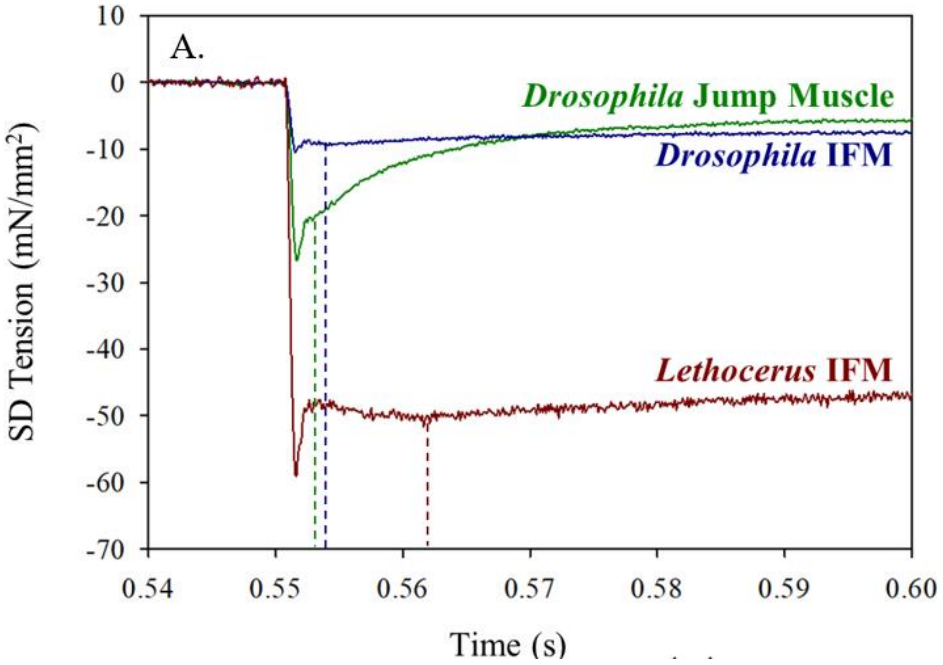

Figure 8: Representative shortening deactivation tension traces from *Drosophila* IFM (blue), *Drosophila* jump muscle (green), and *Lethocerus* IFM (red). Isometric tension levels (F_0) were all set to 0 mM to enable comparisons. Dashed lines indicate where phase 3 amplitudes of shortening deactivation (F_{SD}) were measured for each muscle type. Figure from (51).

Both SA and SD have been hypothesized to work together during cyclical contractions to improve net muscle specific tension and power production, however unlike SA there is a severe lack of information about SD. In measuring power output from a *Cotinus mutabilis* (beetle) IFM, increases in temperature from 25°C to 40°C were shown to increase rates of both SA and SD (43). Two distinct research groups had experimental protocols that included both muscle stretching (SA) and shortening (SD) in

different [Ca^{2+}], one in *Lethocerus* (49) and the other in both *Lethocerus* and *Drosophila* (33), however both articles focused their attention on the effects [Ca^{2+}] had on $F_{SA,}$ leaving F_{SD} unexamined. SD of cardiac tissue is believed to benefit contractions (78) however no direct investigation has provided insight, and to our knowledge there are no studies regarding skeletal muscle. As for now, SD is theorized to work alongside SA and benefit power production, yet more evidence is needed.

2.3 Proposed Mechanisms of Stretch Activation

2.3.1 Early Work

Over the 40+ years of investigation into SA many theoretical models have been proposed for the underlying mechanisms including the thin filament lattice-matching model (88), connecting filament (titin) stretch model (26, 35), filament compliance involving realignment of myosin-binding sites (14, 52), myosin regulatory light chain phosphorylation (18), interacting heads motif (39), and the myosin isoform kinetic model (79). Out of these, the thin filament troponin-bridges model has grown in popularity and is currently considered the accepted model for IFM and cardiac tissue. However, with the addition of evidence suggesting a myosin-based mechanism in skeletal muscle, the underlying components of SA may be muscle-type dependent.

2.3.2 Current Supported Hypothesis

Currently the most accepted hypothesis for the underlying mechanism of SA within IFM and cardiac tissue is the thin filament-based mechanism. This method relies on “troponin-bridges”, in which myosin heads can bind to the thin-filament regulatory protein troponin (10, 62). Typically, in the absence of Ca^{2+}, the tropomyosin-troponin complex formation blocks the binding site of myosin on the actin molecule. In

mammalian skeletal muscle, contractions are dictated by Ca^{2+} release into the myoplasm and their resulting binding to troponin, causing a shape change to the tropomyosin-troponin complex. By quickly freezing IFM during an isometric contraction, ~15% of all cross-bridges were troponin bridges (89). Evidence that this mechanism contributes to IFM's ability to generate stretch-induced specific tension is provided by Perz-Edwards et al., who uses X-ray diffraction to observe *Lethocerus* (water bug) flight muscle during stretch (62). Their working model of troponin bridges is derived from findings of thin-filament elongation, tilting of myosin heads, structural changes to troponin and narrowing of the thick and thin filament during stretching (62). Like myosin, troponin also expresses different isoforms, TnC1 and TnC4, which may also have an impact on muscle's ability to generate specific tension via SA. Investigation of both troponin isoforms in *Drosophila* IFM during a Ca^{2+} activated stretch revealed that only expression of TnC1 resulted in muscle fibers generating isometric tension, power, and F_{SA} (20). When expressed with the TnC4 isoform, fibers did not generate isometric tension or power, and the typical tension transient in response to a stretch was non-existent. This could partially explain the difference in F_{SA} values between insects such as *Drosophila* and *Lethocerus* insects since both species vary in troponin isoforms.

2.3.3 Potential Myosin-Based Mechanism

Revisiting the work done by Zhao & Swank, when *Drosophila* jump muscle was exposed to the IFM isoform and F_{SA} was compared to normal IFM F_{SA}, F_{SA} in the experimental jump muscle expressing IFM was significantly less than the normal IFM (91). These findings show that the IFI does not solely dictate SA properties, and that a potential new, undiscovered mechanism must contribute to the phenomenon in skeletal

muscle. Now with the supporting evidence with F_{SA} increasing in soleus muscle fibers as [Pi] increases (76), a myosin-based mechanism for SA has been proposed. This proposal contains two parts: the first is the mechanism that enables muscles to produce moderate F_{SA} at higher [Pi] in slower contracting myosin isoforms, such as those that compose the soleus muscle. In the presence of Pi, stretching a slower myosin isoform can result with some of the cross-bridges in the strongly bound post-power stroke state to bind with Pi and reverse back to the weakly bound pre-power stroke state. Increasing the number of cross-bridges in the weakly bound state can increase the number of cross-bridges readily available to bind with actin and produce force, which contributes to the observed Phase 3 amplitude. This theory is demonstrated by the green arrow in **Figure 9A**. The second component of this proposed mechanism involves faster myosin isoforms, such as those expressed in the EDL, in which the reversal of the post-power stroke state with Pi occurs less often. Some myosin within these muscle types may be reversible and follow same cross-bridge cycle as the slower myosin isoform (**Figure 9A**); however, the majority are hypothesized to undergo a detachment (purple arrow, **Figure 9B**) without the reversal into the weakly bound pre-power stroke state and must release Pi and adenosine diphosphate (ADP) as well as rebind adenosine triphosphate (ATP) before undergoing another power stroke. This hypothesis, while backed with compelling data, is novel and requires subsequent further examination.

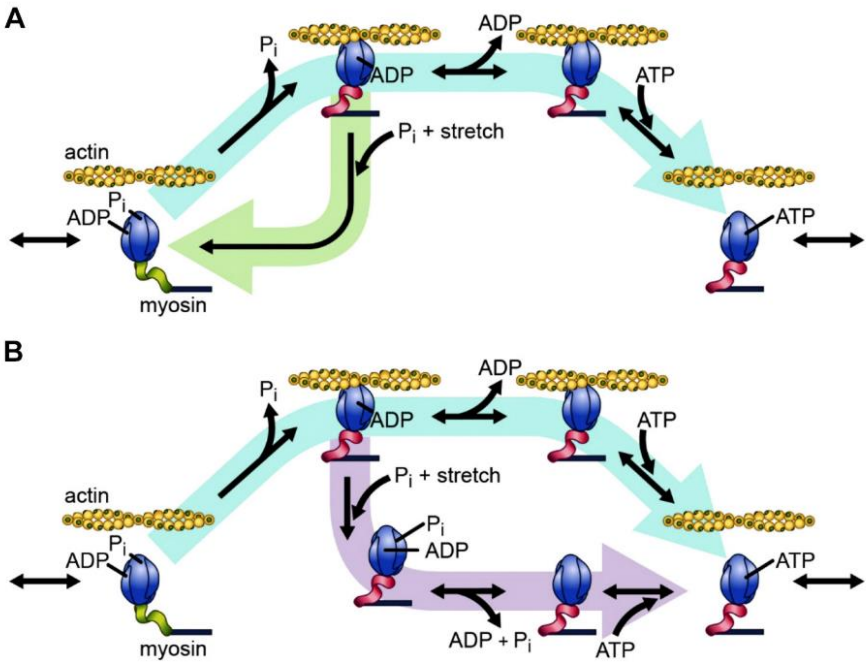

Figure 9: Proposed stretch activation mechanisms for mammalian skeletal muscle fibers. The standard accepted cross-bridge cycle pathway is shown outlined in blue, while the myosin-based proposed pathways for cross-bridges subjected to stretch and Pi are shown outlined in green for soleus (A) and purple for extensor digitorum longus (EDL) (B). The green-colored lever arm of myosin indicates a pre-power stroke state, while the red lever arm indicates a post-power stroke state. Figure from (76).

2.4 Skeletal Muscle Fatigue

2.4.1 Overview

Muscle fatigue is a complex functional characteristic of skeletal muscle, and involves several parameters included neurophysiology, intracellular signaling, bioenergetics, and molecular mechanics (47). Due to the *in-vitro* experiments at the single fiber level this project is proposing, the approach of this paper will be to focus on fatigue at the level of the single myocyte. Therefore, skeletal muscle fatigue is defined as the decreased ability for muscles to generate force or power due to a reduction in contractile velocity and/or specific tension in response to contractile activity (46, 47). Continuous and/or intense muscular activity dictates muscular fatigue, and while both neural and contractile elements contribute to contractile interactions, fatigue is primarily

thought to be attributed to the processes within the muscle itself (2, 46). Whole-body performance is largely due to whole-muscle function, which in turn is due to single muscle fiber performance (13, 55). So, in trying to understand how fatigue impacts whole-muscle and whole-body performance one must take into consideration the changes occurring and the cellular and molecular level. Regarding SA, evidence exists that skeletal muscle F_{SA} is influenced to a degree by Pi (76, 90, 91). Furthermore, increases in F_{SA} with increasing Pi may be fiber-type specific, as seen with increased F_{SA} values in soleus muscle and no change in EDL fibers (76). Due to these recent findings, this literature review will briefly focus on muscular fatigue at the molecular and cellular levels to understand the adaptations during prolonged contractile activity, as a build-up of Pi is a metabolic condition that occurs during repeated muscular contractions. To note, this will not be an in-depth review of muscular fatigue; for that we recommend readers turn to other work (47).

2.4.2 Biochemical Changes *in-vivo*

During muscle contraction, adenosine triphosphate (ATP) is hydrolyzed to form adenosine diphosphate (ADP) and Pi, releasing energy, and in the presence of Ca^{2+} initiating the power stroke. ADP and Pi are by-products of every myosin-actin interaction, and in non-fatiguing conditions the body will resynthesize them back to ATP to maintain homeostasis. During prolonged muscle contractions ATP demand increases, and as the rate of ATP utilization increases so too does the creatine kinase (CK) reaction, ultimately leading to a decline in phosphocreatine (PCr) and a rise in Pi (47). Increased ATP turnover and anaerobic metabolism also contribute to a build-up of hydrogen ions (H^+), which is measured by a drop in intracellular pH. While other metabolites such as

ADP and reactive oxygen species (ROS) or reactive nitrogen species (RNS) build up within the muscle during prolonged contractile activity (12, 16, 84), both Pi and H^+ are suggested to be the primary mechanisms of muscular fatigue. At the cellular level, both Pi and H^+ at higher concentrations (30 mM Pi and pH ~ 6.2) have been shown to impact the myosin-actin cross-bridge cycle (4, 16, 23). *In vivo*, both an increase in Pi and H^+ (signified as a decline in pH) are temporarily correlated with a decline in peak force during a fatiguing protocol of the knee extensor groups (**Figure 10**) (9).

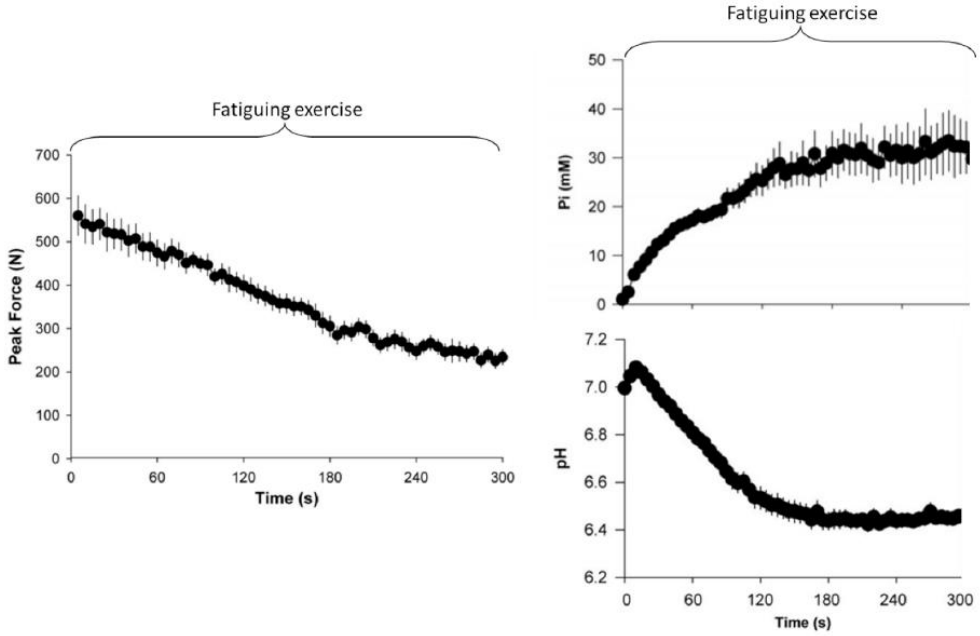

Figure 10: Changes in force, inorganic phosphate (Pi), and H^+ (pH) during fatigue. Changes in peak force, Pi, and pH over time in the quadriceps muscles in 8 young men fatigued with 5 minutes of intermittent maximal isometric single leg knee extensions (3-s contraction, 2-s relaxation). Metabolite concentrations were measured using magnetic resonance spectroscopy. Figure modified from (9).

2.4.3 Classifying fatigue into phases

Both Pi and H^+ build-up quickly within the muscle during repeated contractions, initially rising within a minute and peaking around 2-3 minutes (**Figure 10**) (9, 47).

Evidence exists that suggests intracellular [Ca^{2+}] declines during fatigue (2, 3, 48, 85), which is thought to be related to alterations to the ryanodine receptors (RyR), specific channels along the sarcoplasmic reticulum (SR) that are responsible for the release of Ca^{2+} into the myoplasm (47). Unlike Pi and H^+ the negative effects Ca^{2+} imposes on specific tension generation does not seem to appear as early as the other mentioned metabolites, as in single fiber experiments declines in [Ca^{2+}] occur in the later stages of the contraction period (**Figure 11**). [Ca^{2+}] actually increases during the early fall in specific tension during fatiguing contractions (**Figure 11B:** *a* to *b*) (2, 48). As stimulation frequency progresses the decline in specific tension accelerates, which is accompanied by a decline in [Ca^{2+}] (**Figure 11B**: *c* to *d*).

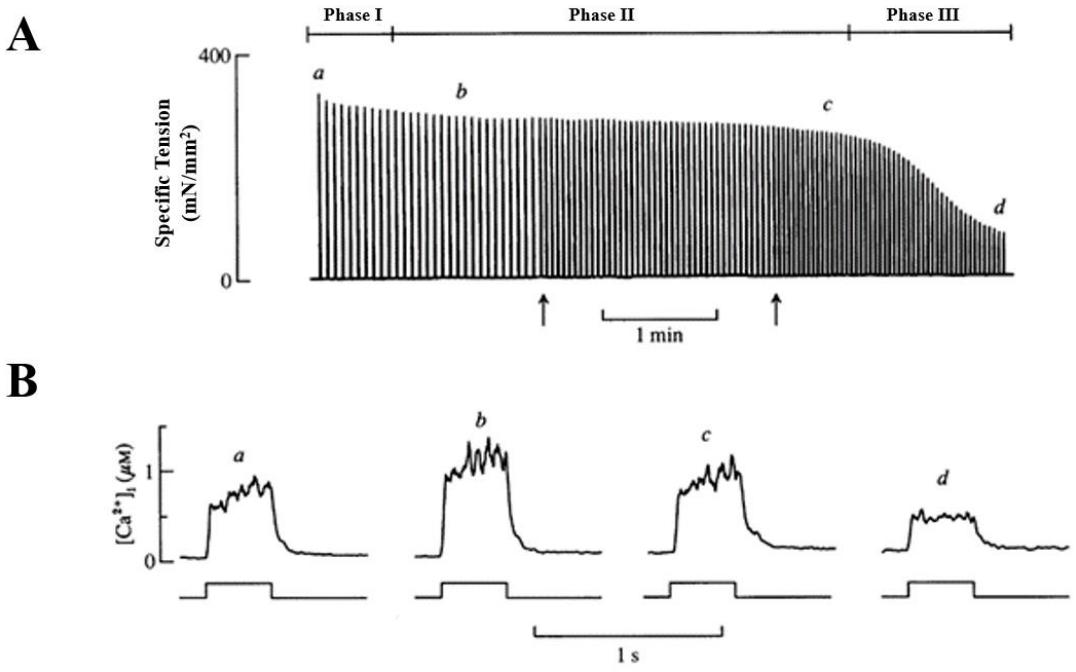

Figure 11: Records of specific tension and [Ca^{2+}] obtained in a single mouse skeletal muscle fiber during a fatigue run. A – Specific tension record where each vertical line represents a 350 ms tetanus at 100 Hz. B - [Ca^{2+}] records (measured with indo-1) from selected tetani; periods of stimulation are indicated below records. Phase I is the early fall of specific tension down to about 85 % maximum, which occurs in 5-10 tetani. Phase II is the slower, linear component of decline, which follows Phase I. Phase III is the accelerated decline of specific tension, which terminates Phase II. Observe that tetanic [Ca^{2+}] increases slightly during Phase I, remains high during Phase II, and falls markedly during Phase III. Figure from (2).

Declines in intracellular [Ca^{2+}] and the metabolic by-product of Pi and H^+ accumulation work in harmony to further impact cross-bridge function (16, 58), particularly by decreasing myofilament sensitivity to Ca^{2+} (16, 17, 23, 58, 81). Both Pi and H^+ have been shown to decrease Ca^{2+} sensitivity, albeit via separate mechanisms. Acidosis is believed to decrease the affinity of Ca^{2+} for its binding sites on troponin (16, 22, 50, 59, 60), while Pi is thought to decrease overall thin filament activation by directly decreasing the number of strongly bound myosin heads at any given moment (15–17, 53).

Hence, the large decrements in force production seen during extended muscle contractions is thought to be explained by the combination of metabolic by-products, reduced free Ca^{2+} within the myoplasm, and a decrease in the myofilament sensitivity to Ca^{2+}.

As such, the biochemical contributions to muscular fatigue can be classified into two phases: an initial, metabolite-induced stage, in which Pi and H^+ accumulation due to heighted ATP utilization directly impede the cross-bridge cycle, and a second, Ca^{2+} influenced stage, where following Pi and H^+ accumulation, declines in both [Ca^{2+}] and sensitivity further contribute to the reductions in force production. This classification scheme is demonstrated in **Figure 12,** where the arrows indicate direction of time. The decline in maximal force production, primarily due to Pi and H^+ is shown by the first arrow, while a decline in Ca^{2+} sensitivity is shown by the rightward shift of arrow 2. The dashed line demonstrates the initial rise and resulting fall of the concentration of Ca^{2+} during fatigue.

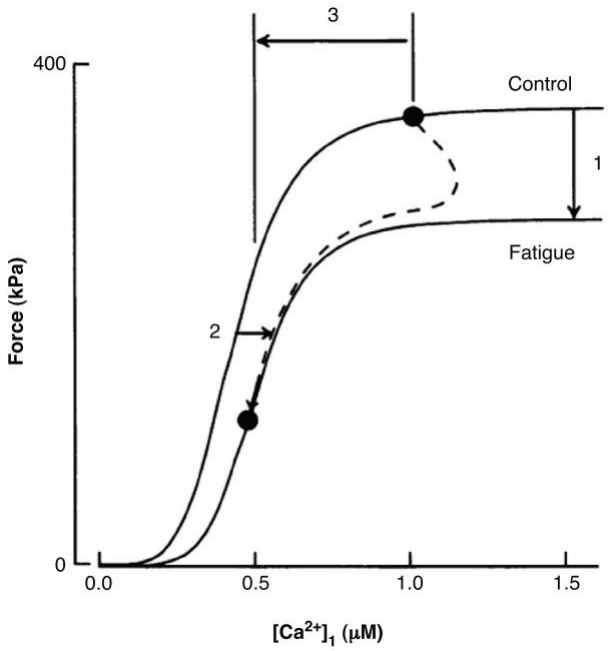

Figure 12. A plot of force versus [Ca^{2+}] summarizing the mechanisms involved in the reduction of isometric force in fatigue: (1) reduced maximum force; (2) reduced myofibrillar Ca^{2+} sensitivity; and (3) reduced tetanic [Ca^{2+}]. The normal pattern during fatigue is schematically illustrated by the dashed line. The arrow shows the direction of time. Figure from (2).

2.5 Summary

SA is a mechanical response to a physical stimulus that is present in all muscle. Research has existed for the last 7 decades highlighting the amplitude of this phenomenon's importance during insect flight. *Drosophila melanogaster* and other insects have evolved to rely on the repeated stretching of two major muscles, the Dorsal Ventral and Dorsal Longitudinal Muscles to produce specific tension required for locomotion. Evidence of SA in cardiac tissue seen aiding in blood ejection soon followed. Skeletal muscle, as mentioned previously, was discovered to demonstrate this response two decades after the initial discovery, and, unlike both IFM and cardiac tissue, SA did not have an immediate apparent physiological importance. Kinetics of SA were found to be influenced by certain factors such as temperature and fiber type, yet F_{SA} was

still miniscule to total force production compared to F_0 until recently. New evidence has emerged suggesting a potential relevance in skeletal muscle, as seen with F_{SA} increasing in soleus muscle fibers in the presence of Pi. The possibility of SA aiding in specific tension production for slower contracting muscle fibers in environments of high [Pi] is exciting, as the soleus muscle contributes to locomotion in both mice and humans and could potentially utilize the delayed tension increase in scenarios of Pi buildup, such as muscular fatigue during prolonged locomotion. However, muscular fatigue is a vast and complex characteristic of skeletal muscle, and metabolically incorporates more than just Pi. Understanding the response of SA within simulated conditions of peripheral fatigue, where the major force-inhibiting metabolites such as Pi and H^+ as well as these metabolites' influences on $[Ca^{2+}]$ must be accounted for to provide any insight into physiological relevance within skeletal muscle.

CHAPTER 3

METHODS

3.1 Introduction

This study aimed to investigate the phenomenon of SA, a delayed increase in specific tension following a rapid stretch of a Ca^{2+} activated muscle fiber, during simulated *in vitro* conditions of muscular fatigue to identify whether this phenomenon has physiological importance within skeletal muscle. Single muscle fibers were extracted from the soleus and EDL muscles from female C57BL/6NJ mice and exposed to three distinct experimental conditions: Active (control – pCa 4.5, pH 7, 5 mM Pi, 5 mM ATP), High Ca^{2+} Fatigue (pCa 4.5, pH 6.2, 30 mM Pi, 5 mM ATP), and Low Ca^{2+} Fatigue (pCa 5.1, pH 6.2, 30 mM Pi, 5 mM ATP). Within each experimental condition F_0, F_{SA}, and t_3 were measured and F_{SA}/F_0 was calculated.

3.2 Mice

This study used tissue from the soleus and EDL muscles from female C57BL/6NJ mice, sacrificed at 8-15 weeks old (~10% of their lifespan). Justification for using female mice only is due to no current data suggesting sex-specific differences regarding SA within skeletal muscle. The mice used in this investigation also served as the control group in Dr. Mager's experiments, as approved by the University of Massachusetts Institutional Animal Care and Use Committee. All mice were raised under standard housing conditions at room temperature and supplied with breeder's chow ad libitum.

3.3 Experimental Preparation

3.3.1. Location

Dissections of soleus and EDL muscles were performed in Dr. Mager's Veterinary & Animal Sciences Laboratory at the University of Massachusetts Amherst in

the Integrated Life Sciences Building, Room 455. Further muscle bundle preparations, single fiber preparations and functional analysis measures were completed in the Muscle Biology Laboratory at the University of Massachusetts, Amherst in Totman Physical Education Building, Room 140E.

3.3.2. Experimental Apparatus

A custom built muscle mechanics apparatus was used, as previously described (56). Briefly, an aluminum bath plate of 13 wells (~100 µl each) was made to hold experimental solutions and a single large chamber (~450 µl) for mounting the fiber onto the force and linear motor hooks. Once a fiber was mounted in solution, the bath plate was lowered, moving the fiber out of the chamber, and slid horizontally within a metal trough, underneath the fixed motor and force gauge, allowing the fiber to be moved (~1 s) between chambers and different solutions. The bathing solutions were maintained at a constant temperature by circulating cooling solution through channels milled into the chamber walls. The bathing solution assembly is mounted to an inverted microscope (Zeiss Invertiscope) with a video camera (BFLY-U3-23S6m-C, Point Grey Research Inc., Richmond, British Columbia, CA) and custom video analysis software (69) that enabled precise measurements of fiber dimensions and sarcomere length.

3.3.3 Experimental Solutions

All solutions used for dissection processing and single fiber experiments were calculated using the equations and stability constants according to Godt and Lindley (34), as described previously (56). Dissecting solution was 20 mM *N*,*N*-bis[2-hydroxyethyl]-2-aminoethanesulfonic acid (BES), 5 mM ethylene glycol-bis(2-amino-ethylether)-N,N,N',N'-tetraacetic acid (EGTA), 5 mM MgATP, 1 mM free Mg^{2+}, 1 mM

dithiothreitol (DTT) and 0.25 mM Pi with pH 7.0 and at pCa 8.0. Skinning solution was 170 mM potassium propionate, 10 mM imidazole, 5 mM EGTA, 2.5 mM $MgCl_2$, 2.5 mM Na_2H_2ATP and protease inhibitor (Roche) with pH 7.0. Storage solution was identical to skinning solution, but with 1 mM sodium azide. Relaxing solution as the same as dissecting solution, but with 5 mM P_i, 15 mM creatine phosphate (CP) and 300 µl/ml of creatine phosphokinase (CPK). Pre-activating solution was the same as relaxing solution, except at an EGTA concentration of 0.5 mM. Active solution was the same as relaxing solution, but at pCa 4.5. Relaxing and Active solutions were mixed to achieve different pCa concentrations. High Ca^{2+} Fatigue was the same as Active except with a pH of 6.2 and a Pi level of 30 mM. Low Ca^{2+} Fatigue is the same as High Ca^{2+} Fatigue but with a pCa value of 5.1. All solutions were adjusted to an ionic strength of 175 mEq using sodium methane sulfate.

3.3.4. Muscle Tissue Processing

Muscle tissue processing has been described previously (56), with adaptations for rodent tissue. After dissection, soleus and EDL muscles were tied to glass rods and placed in skinning solution, a low Ca^{2+} solution that begins the removal of the muscle fibers' external membrane (86), for 24 hr at 4°C and then stored in storage solution with glycerol (50% v/v) at -20°C. Addition of glycerol prevents solution from freezing and damaging the fibers as well as creating an osmotic pressure gradient to further permeabilize the muscle fibers' external membrane. All mechanical measurements occurred within 4 weeks of the dissection.

3.3.5. Preparation of Single Fibers

Muscle tissue processing has been described previously (56), with adaptations for rodent tissue. On the day of the experiment, a section of either the soleus or EDL was removed with scissors to create a muscle fiber bundle and placed in a dissecting solution with 1% Triton X-100 for 30 minutes at 4°C to remove more of the sarcolemma and sarcoplasmic reticulum (75). This stage is often referred to in the lab as "skinning". After initial skinning, the muscle bundle was then transferred to a dish containing dissecting solution, cut ~1 mm in length and then manually separated for single muscle fibers using forceps. Aluminum T-clips were placed at both ends of the fiber and top and side diameters were measured in dissecting solution to estimate the height-to-width ratio. Individual muscle fibers with T-clips were then transferred to the skinning dish for a second time (dissection solution with 1% v/v Triton X-100) for 30 minutes at 4°C to ensure no remnants of the sarcolemma are intact. Once demembranated a second time, all prepared muscle fibers were stationed in dissecting solution until ready for experiments.

3.3.6 Single Fiber Mechanical Measurements

Calcium-Activated Specific Tension (F_0). Single fibers were transferred to the experimental apparatus containing relaxing solution at 15°C and mounted to the experimental apparatus by sliding the holes in the T-clips over the hooks attached to a piezo actuator linear motor (P-841.10, Physik Instrumente, Auburn, MA) and an Akers strain gauge (AE-801, SensorOne, Sausalito, CA) (**Figure 13**). Sarcomere length was adjusted to ~2.5 µm with tension baseline recorded, transferred to Pre-activating solution (same as relaxing, except EGTA is decreased to 0.5 mM) for 30 seconds, and then transferred to Active solution where specific tension was measured at the plateau. Reasoning for measuring specific tension at 15°C is two-fold; 1) activation at 15°C

prepares the fiber for the higher temperature of 25°C and 2) allows for better visibility of sarcomeres (Muscle Biology Lab (MBL), unpublished observations). After initial activation, fiber was returned to Relaxing solution where temperature was set to 25°C. Sarcomere length was set to 2.65 µm and CSA was determined by measuring the width of the fiber on the apparatus' compound microscope and estimating the height using the previously determined height-to-width ratio, which presumes the fiber's CSA is elliptical. The fiber was then slackened completely, force gauge zeroed, then pulled back to its original length and allowed to equilibrate for 1 minute. After 1 minute the relaxed specific tension was measured and the fiber was transferred to Pre-activating solution (same as relaxing, except EGTA is decreased to 0.5 mM) for 30 seconds. At this point, fibers were placed into Active solution, maximal F_0 measured at its plateau, then placed back into Relaxing solution and ready for step analysis.

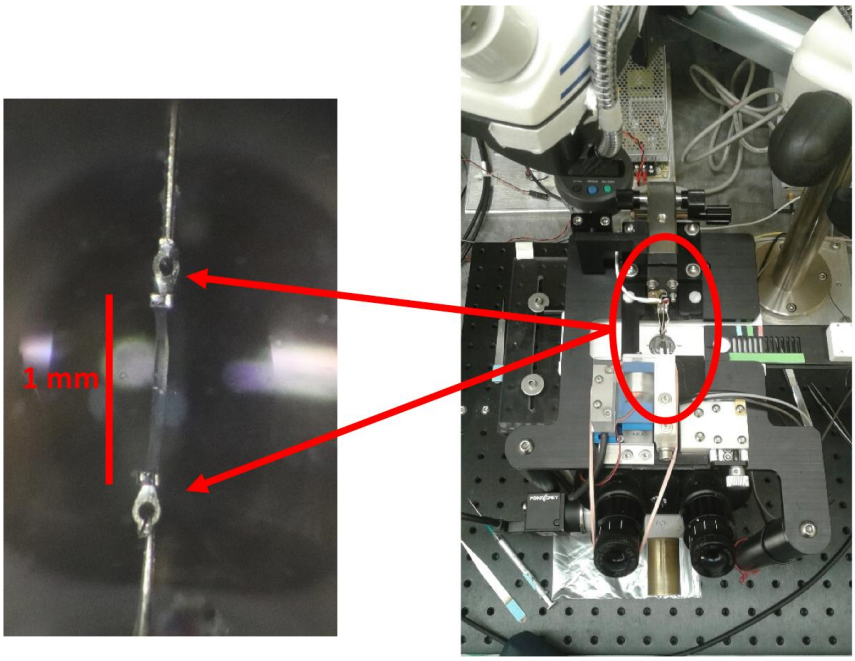

Figure 13. Sinusoidal analysis rig. Left: Magnified view of single muscle fiber with T clipped ends mounted on hooks connected to the force gauge (top) and length motor (bottom). Right: Top view of sinusoidal analysis rig. Figure from Muscle Biology Lab, UMass Amherst.

Stretch-Activated Specific Tension (F_{SA}) via Trapezoidal Step Length. Step experiments have been described previously (76), with modifications made in order to investigate SA's opposite yet symmetrical response, SD. Following maximal F_0 at 25°C, the fiber was transferred to Relaxing solution and a relaxed specific tension transient was collected by stretching the fiber by 0.5% of its optimal muscle length (ML) over a period of 4 ms. The fiber was held at this stretched length for 2 s and then returned to its original length over a period of 4 ms. This rapid stretch-hold-release pattern is often referred to as a "trapezoidal stretch", as the length trace has a trapezoidal/rectangular pattern. The fiber was placed into Pre-activating solution for 30 s, then into Low Ca^{2+} Fatigue solution and specific tension was measured until a plateau was reached. SA was induced by repeating the same length step (0.5% over 4 ms, 2-s hold, 4 ms return) in Low Ca^{2+} Fatigue. The fiber was transferred (without returning it to Relaxing solution) from Low Ca^{2+} to High Ca^{2+} Fatigue to Active, with F_0 and resulting step experiment conducted at each condition. Following Active, fibers were placed back into Relaxing solution where sarcomere length was checked. If sarcomere length was below 2.65 µm, fibers were stretched back to 2.65 µm, slacked and the force gauged zeroed, re-lengthened and allowed to equilibrate for 1 minute. Relaxed specific tension was re-measured, fiber placed into Pre-activating solution for 30 sec, then placed in Active solution where F_0 and resulting step experiment was conducted for a second time. Reasoning for conducting measurements in Active condition twice was to check for fiber run down. Fibers were exposed to experimental solutions from high to low [Pi] so that isometric tension starts low and increases throughout the protocol, which in theory should prolong fiber stability. To measure fiber stability, specific tension was measured pre- and post-length step in

each of the three experimental conditions. At the end of the length-step protocol, specific tension and slacked specific tension in Relaxing solution was measured and compared to baseline values to control for fiber drift.

3.3.7 Myosin Heavy Chain Isoform Composition

Following single fiber mechanical analysis, single fibers were placed in 30 ul loading buffer, heated for 2 min at 65°C and stored at -80°C until determination of MHC isoform composition by sodium dodecyl sulfate-polyacrylamide gel electrophoresis (SDS-PAGE) to identify fiber types, as previously described (56) with modifications. Resolving gel was comprised of 8% acrylamide/bis-30% glycerol (w/v) and gels were run at 70 V for 1 hour followed by 275 V for 26 hours.

3.4 Analysis of Stretch Activation

Magnitude of Stretch Activation, F_{SA}. F_{SA} was determined post data collection using a custom-built Shiny App through R and RStudio (R Core Team, 2021). A single force trace from any given experimental condition was loaded into the software, where the entire SA response was selected. Once selected, the program would compute a running mean of 2 ms over the entire force trace using RcppRoll::rollmeanl and the max force value during the selected region would be exported. Max SA force value would then be normalized to CSA in Excel to create F_{SA}. This process was repeated for all fibers within each of the three experimental conditions.

Timing of Stretch Activation, t_3. To calculate the time of when SA was occurring, the force response was fitted to the sum of three exponential curves (*Eq 1*), with r_2 the rate of rapid force decrease that occurs during Phase 2, r_3 the rate of delayed increase in force that occurs during Phase 3, and r_4 the rate of force decay that occurs during Phase 4:

$$F = a_2e^{(-r2t)} + a_3[1-e^{(-r3t)}] + a_4e^{(-r4t)} \quad (1)$$

with t_3 being determined by taking the inverse of r_3. If SA was not visibly apparent, the force response was also fitted to the sum of two exponential curves *(Eq 2),* where only r_2 and r_4 was included:

$$F = a_2e^{(-r2t)} + a_4e^{(-r4t)} \quad (2)$$

and compared to the fit from *Eq 1*. If the force trace had a similar and/or better fit using *Eq 2* over *Eq 1,* then SA was deemed to not have occurred.

3.5 Statistics

Data are expressed as mean ± SE and differences were considered significant at $P \leq 0.05$. As there were multiple observations within the same mouse, main effects were determined using a repeated-measures linear mixed model was used, with a random effect to account for grouping of observations within mice and a repeated effect to account for the between-mice factor (i.e., Active group vs. High Ca^{2+} Fatigue vs. Low Ca^{2+} Fatigue). Tukey's post-hoc test was performed to determine pairwise differences between the three experimental conditions. All statistical analyses were conducted using custom written R scripts (https://github.com/19PWoods/Masters) (R Core Team, 2021).

3.6 Proof of Concept

As the SA response has, to my knowledge, not been examined under fatiguing conditions, I performed some initial experiments to test some of my hypotheses. Trapezoidal length step experiments (as described in **Section 3.3.6 Single Fiber Mechanical Measurements**) were applied to single soleus muscle fibers (n=7) in Active (pCa 4.5, pH 7, 5 mM Pi, 5 mM ATP) and Fatigue 6.6 (pCa 6.6, pH 6.2, 30 mM Pi, 5 mM ATP) conditions, which have been labelled "Active" and "Fatigue" (**Figure 14**). F_{SA}

was selected in both conditions by visual indication of the peak in the secondary specific tension increase. In scenarios where Phase 3 was not obvious, F_{SA} was chosen based on the time point of Phase 3 in other fibers of the same fiber types. Sinusoidal analysis was performed following step experiments to distinguish fiber types as either type I or II, as the dip in the viscous modulus, which is related to $2\pi b$, has proven to be fairly accurate for predicting pure fiber types relative to gel electrophoresis (MBL, unpublished observations). All preliminary data shown is composed of type II fibers collected from the soleus muscle.

Figure 14A shows F_0 for both Active and Fatigue conditions. As expected, F_0 was significantly lower (100 ± 12 mN/mm^2) in Fatigue compared to Active (204 ± 27 mN/mm^2). F_{SA} was similar for both Active and Fatigue (**Figure 14B**), F_{SA}/F_0 ~20% higher in Fatigue (~36%) vs. Active (~16%) conditions (**Figure 14C**). While these data are preliminary, the vast difference in F_{SA}/F_0 observed is similar to that at high Pi (76), leaving the expectation of statistical differences being observed between the experimental conditions for the trapezoidal step experiments.

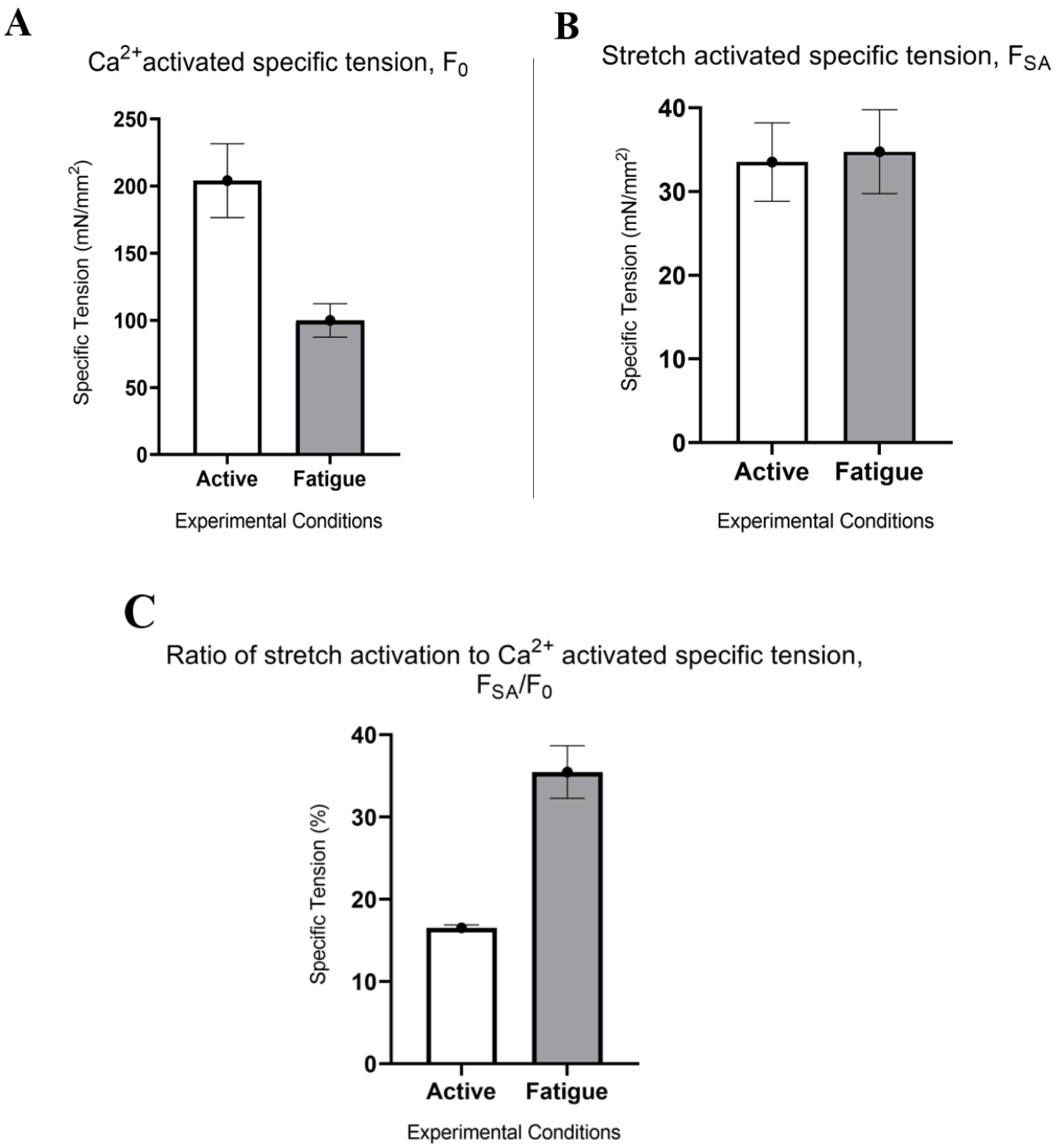

Figure 14: Trapezoidal length step experiments (0.5% of ML) performed on single muscle fibers from the soleus muscle. A) Ca^{2+} activated isometric specific tension (F_0). B) Stretch activated specific tension, F_{SA}. C) Ratio of stretch activated to Ca^{2+} activated specific tension (F_{SA}/F_0). Figure from (Woods, Swank, Miller 2021. Unpublished).

CHAPTER 4

RESULTS

4.1 Introduction

This study examined the effects of simulated *in vitro* initial- and secondary-stages of muscular fatigue (High Ca^{2+} Fatigue and Low Ca^{2+} Fatigue) on F_{SA} compared to Active in single mouse skeletal muscle fibers. We tested 89 total fibers from the soleus (n=53) and EDL (n=36) muscles from female C57BL/6NJ mice (N=8), aged 12-15 weeks. SDS-PAGE analysis resulted in the classification of the 89 total fibers into one of six MHC isoforms: MHC I (n=14), MHC IIA (n=32), MHC IIAX (n=7), MHC IIX (n=11), MHC IIXB (n=6), and MHC IIB (n=19). Due to the small sample size of MHC IIAX and IIXB, this thesis will only focus on the results from the four pure MHC isoforms, MHC I, IIA, IIX, and IIB. Means and SE for F_0, F_{SA}, F_{SA}/F_0, and t_3 are presented in **Table 1** and shown graphically, including statistical analysis, in **Figures 15**, **16**, **18**, and **19**.

MHC	F_0 (mN/mm$_2$)			F_{SA} (mN/mm$_2$)			$F_{SA}F_0$ (%)			r_3 (ms)		
	Active	High Ca^{2+} Fatigue	Low Ca^{2+} Fatigue	Active	High Ca^{2+} Fatigue	Low Ca^{2+} Fatigue	Active	High Ca^{2+} Fatigue	Low Ca^{2+} Fatigue	Active	High Ca^{2+} Fatigue	Low Ca^{2+} Fatigue
I (n = 14)	178 ± 20	130 ± 20*	102 ± 20**	7 ± 2	---	---	4 ± 1	---	---	9.7 ± 1.3	---	---
IIA (n = 32)	183 ± 18	129 ± 13**	101 ± 12$^{**\#\#}$	27 ± 2	39 ± 3**	32 ± 6	14 ± 1	32 ± 2**	35 ± 2**	54.8 ± 2.0	22.4 ± 4.4	11.4 ± 5.0
IIX (n = 11)	171 ± 14	119 ± 12**	76 ± 14$^{**\#\#}$	30 ± 4	38 ± 6	32 ± 7	17 ± 2	31 ± 3**	41 ± 4$^{**\#\#}$	128 .1 ± 10.7	88.0 ± 24.0	92.6 ± 25.7
IIB (n = 19)	156 ± 17	109 ± 14**	52 ± 9$^{**\#\#}$	32 ± 4	37 ± 4	21 ± 4$^{**\#\#}$	20 ± 1	35 ± 1**	44 ± 1$^{**\#\#}$	366.0 ± 42.5	418.0 ± 67.3	394.0 ± 90.2

Table 1: Values are means ± SE. Experimental conditions: Active (pCa 4.5; 5 mM Pi; pH 7.0), High Ca^{2+} Fatigue (pCa 4.5; 30 mM Pi; pH 6.2), Low Ca^{2+} Fatigue (pCa 5.1; 30 mM Pi; pH 6.2). Significant pairwise differences indicated by *P<0.05 vs. control; **P<0.01 vs. control; $^{\#\#}$P<0.01 vs. High Calcium Fatigue.

4.2 Single Fiber Mechanical Measurements

Calcium-activated specific tension. F_0 decreased from Active to High Ca^{2+} Fatigue to Low Ca^{2+} Fatigue in all four MHC isoforms, except for High Ca^{2+} Fatigue to Low Ca^{2+} Fatigue in MHC I fibers (**Table 1** and **Figure 15**). On average, when normalized to the Active condition, fibers produced 71 ± 1% and 48 ± 5% of their F_0 in High Ca^{2+} Fatigue and Low Ca^{2+} Fatigue.

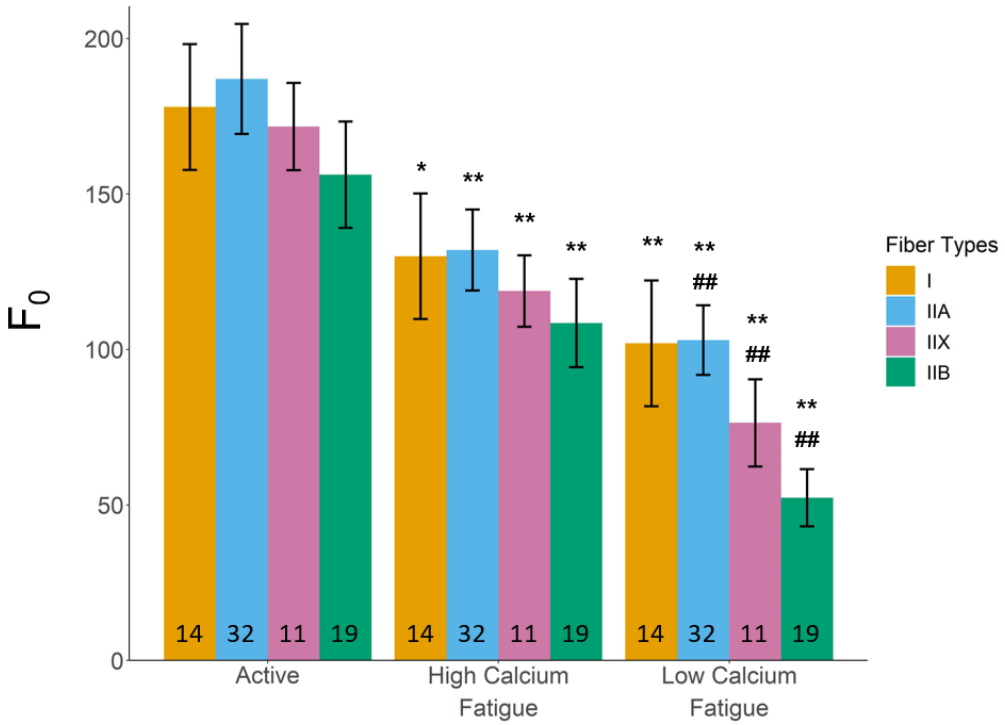

Figure 15: Calcium-activated specific tension (F_0) performed under Active (pCa 4.5; 5 mM Pi; pH 7.0), High Calcium Fatigue (pCa 4.5; 30 mM Pi; pH 6.2) and Low Calcium Fatigue (pCa 5.1; 30 mM Pi; pH 6.2) in myosin-heavy chain (MHC) I, IIA, IIX, and IIB single muscle fibers. Numbers of fibers (n) are indicated at the bottom of each bar graph. Significant pairwise differences indicated by *P<0.05 vs. control; **P<0.01 vs. control; ##P<0.01 vs. High Calcium Fatigue.

Stretch-activated specific tension. The F_{SA} response under fatiguing conditions, unlike F_0, was fiber-type dependent (**Table 1** and **Figure 16**). MHC I fibers displayed a

SA response under Active conditions, but no measurable F_{SA} was found under either fatiguing condition. MHC IIA fibers had a similar SA response in Active and Low Ca^{2+} Fatigue but was higher than Active in High Ca^{2+} Fatigue. Notably, MHC IIA fibers saw a reduction in the number of fibers producing a noticeable F_{SA} from Active (n=32, 100%) to High Ca^{2+} Fatigue (n = 28, 88%) to Low Ca^{2+} Fatigue (n = 8, 25%). MHC IIX fibers showed a similar F_{SA} in Active, High Ca^{2+} Fatigue, and Low Ca^{2+} Fatigue. MHC IIB had a similar maintenance of F_{SA} in Active and High Ca^{2+} Fatigue, however F_{SA} decreased in Low Ca^{2+} Fatigue.

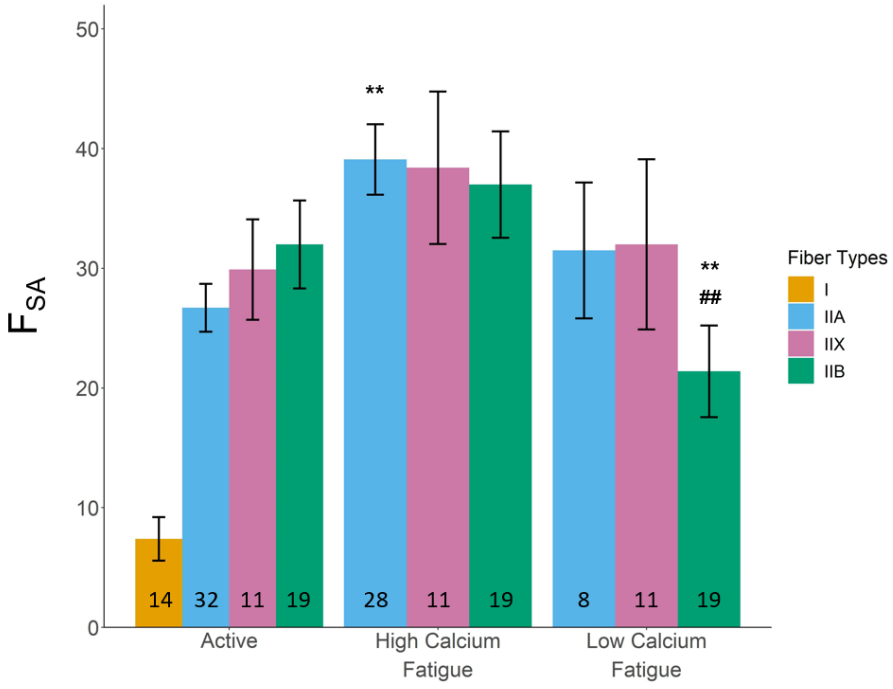

Figure 16: Stretch-activated specific tension (F_{SA}) performed under Active (control – pCa 4.5; 5 mM Pi; pH 7.0), High Calcium Fatigue (pCa 4.5; 30 mM Pi; pH 6.2) and Low Calcium Fatigue (pCa 5.1; 30 mM Pi; pH 6.2) on myosin-heavy chain (MHC) I, IIA, IIX, & IIB single muscle fibers. Numbers of fibers (n) are indicated at the bottom of each bar graph. Significant pairwise differences indicated by *P<0.05 vs. control; **P<0.01 vs. control; $^{\#\#}$P<0.01 vs. High Calcium Fatigue.

Stretch-to-Calcium-activated specific tension. To get a better understanding of SA's contribution to specific tension production, F_{SA} was normalized to F_0. F_{SA}/F_0 increased from Active to High Ca^{2+} Fatigue to Low Ca^{2+} Fatigue in fast-contracting fibers, except for MHC IIA fibers where F_{SA}/F_0 was similar under fatiguing conditions (**Figure 17**). MHC I fibers only produced F_{SA} under Active conditions, so F_{SA}/F_0 could be calculated for this condition alone.

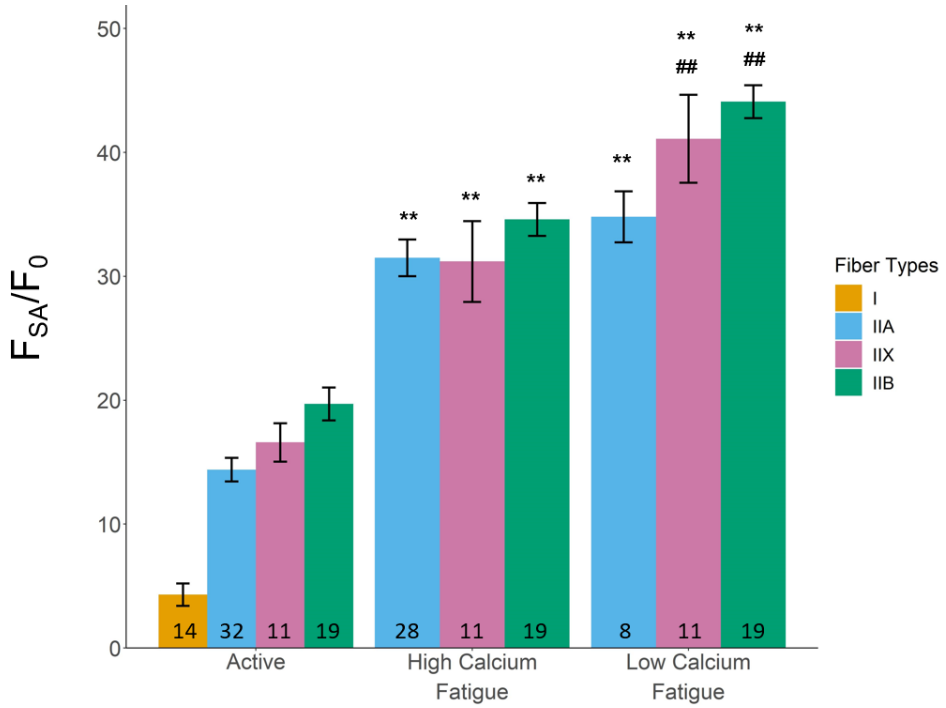

Figure 17: Stretch-activated specific tension (F_{SA}) normalized to calcium-activated specific tension (F_0, F_{SA}/F_0) under Active (control – pCa 4.5; 5 mM Pi; pH 7.0), High Calcium Fatigue (pCa 4.5; 30 mM Pi; pH 6.2) and Low Calcium Fatigue (pCa 5.1; 30 mM Pi; pH 6.2) on myosin-heavy chain (MHC) I, IIA, IIX, & IIB single muscle fibers. Numbers of fibers (n) are indicated at the bottom of each bar graph. Significant pairwise differences indicated by *P<0.05 vs. control; **P<0.01 vs. control; $^{\#}$P<0.01 vs. High Calcium Fatigue.

Rate of Stretch Activation. r_3 decreased from Active to High Ca^{2+} Fatigue to Low Ca^{2+} Fatigue in MHC IIA fibers. Both MHC IIX and IIB rates were similar between the

three conditions. In MHC I fibers, SA was produced under Active conditions, so r_3 could be calculated for this condition alone.

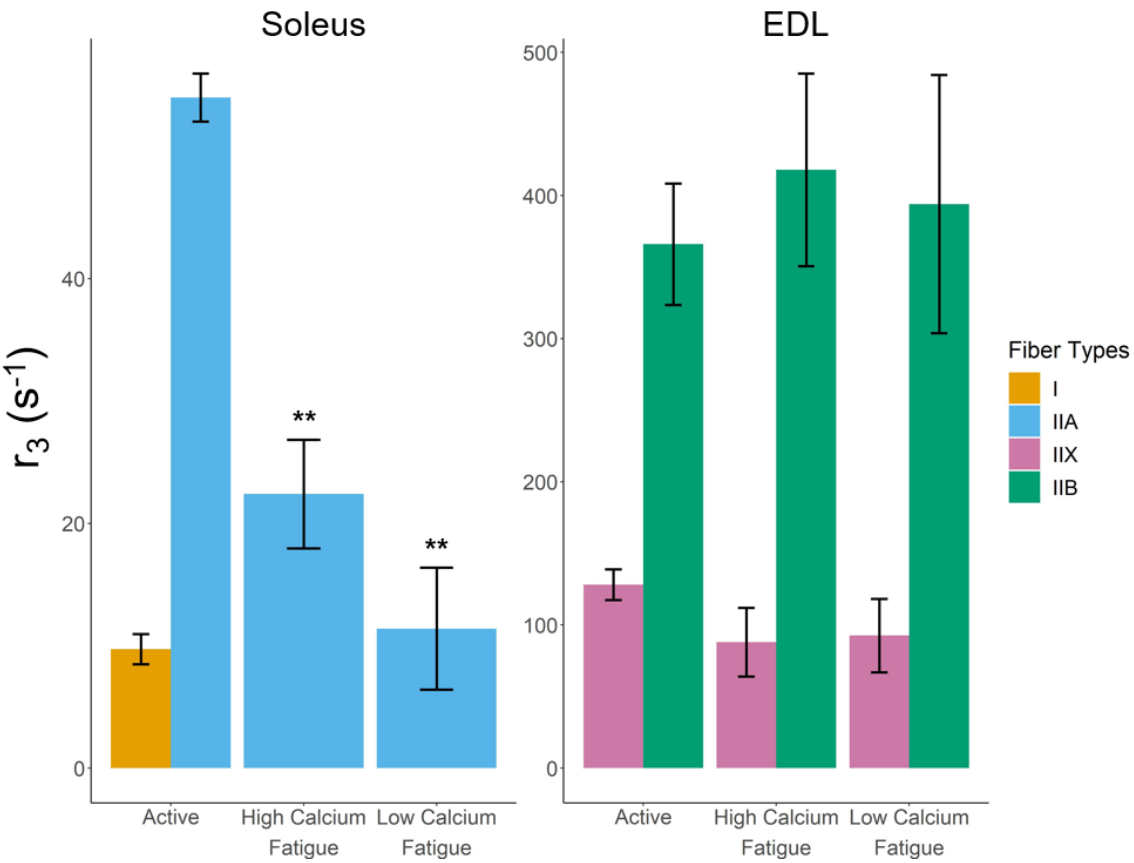

Figure 18: Rate of F_{SA} (r_3) under Active (control – pCa 4.5; 5 mM Pi; pH 7.0), High Calcium Fatigue (pCa 4.5; 30 mM Pi; pH 6.2), and Low Calcium Fatigue (pCa 5.1; 30 mM Pi; pH 6.2) in MHC I, IIA, IIX, & IIB single muscle fibers. Data has been separated by muscle group. Numbers of fibers (n) are indicated at the bottom of each bar graph. Significant pairwise differences indicated by *P<0.05 vs. control; **P<0.01 vs. control; $^{\#}$P<0.01 vs. High Calcium Fatigue.

Changes in the force response between conditions. The average force trace in response to a stretch under each experimental condition for the four MHC isoforms is depicted in **Figure 19**. MHC I fibers in the Active condition showed a clear increase in force after stretch, or F_{SA}, while the High Ca^{2+} and Low Ca^{2+} Fatigue only showed a decay in force over time (**Figure 19A**). The decay in force for fatiguing conditions was

best fit using two exponentials, compared to the three used when F_{SA} was present, providing further evidence that MHC I fibers did not have a stretch activation response under fatiguing conditions. In general, fast-contracting fibers showed a clear stretch activation response for each experimental condition, except for MHC IIA fiber at Low Ca^{2+} Fatigue where the response was very modest (**Figure 19B-D**).

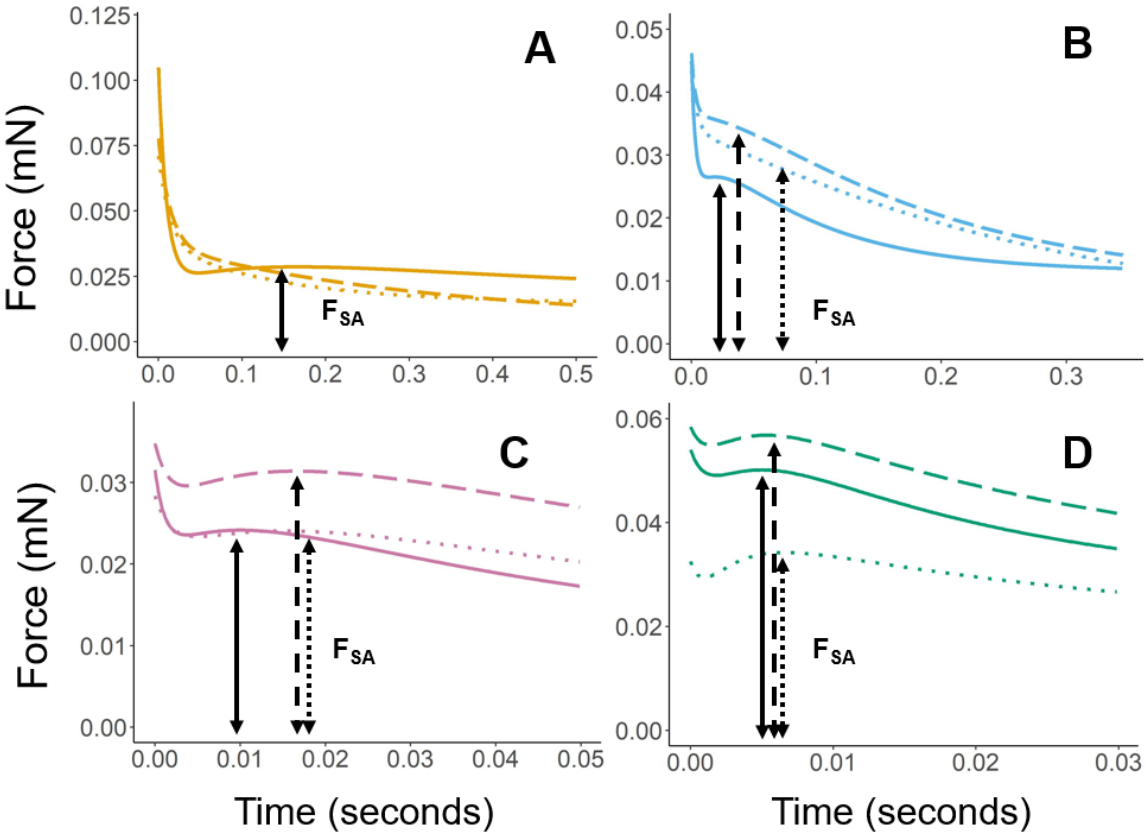

Figure 19: Average Force (mN) trace following a 0.5% muscle length step under Active (solid), High Ca^{2+} Fatigue (long dash), and Low Ca^{2+} Fatigue (dotted line) in: *A*, MHC I fibers; *B*, MHC IIA fibers; *C*, MHC IIX fibers; *D*, MHC IIB fibers. Each trace consists of Phase 2, Phase 3 (if present), and a truncated Phase 4. For each condition, if stretch activation was present **F_{SA}** indicates the magnitude of the stretch activated response for each condition.

CHAPTER 5

DISCUSSION

5.1 Introduction

This study aimed to 1) Determine SA's response during simulated conditions of the initial, metabolite induced phase of muscular fatigue (30 mM Pi, pH 6.2, labeled "High Ca^{2+} Fatigue") and 2) compare the contribution of SA to total specific tension during the initial vs secondary, Ca^{2+} induced phase (30 mM Pi, pH 6.2, pCa 5.1, labeled "Low Ca^{2+} Fatigue") of muscular fatigue in soleus and EDL muscle fibers. **Table 2** summarizes the results of this study. For each MHC isoform SA was observed under Active conditions, while only the fast-contracting isoforms exhibited a SA response under fatiguing conditions (MHC IIA, IIX, and IIB). Interestingly, within the fast-contracting isoforms F_{SA} was typically similar between conditions, which is in stark contrast to fatigue's known impact on F_0. The contrast is even more apparent when looking at $F_{SA}/F_{0,}$ which had a 92 ± 4% and 137 ± 5% greater ratio in High and Low Ca^{2+} Fatigue compared to Active.

MHC	F_0		Phase 3 Observed		F_{SA}		F_{SA}/F_0		r_3	
	High Ca^{2+} Fatigue	Low Ca^{2+} Fatigue	High Ca^{2+} Fatigue	Low Ca^{2+} Fatigue	High Ca^{2+} Fatigue	Low Ca^{2+} Fatigue	High Ca^{2+} Fatigue	Low Ca^{2+} Fatigue	High Ca^{2+} Fatigue	Low Ca^{2+} Fatigue
I	↓	↓↓	0	0	---	---	---	---	---	---
IIA	↓	↓↓	↓	↓↓↓↓	↑↑	↔	↑↑↑↑↑↑	↑↑↑↑↑↑↑	↓↓↓	↓↓↓↓
IIX	↓	↓↓	↔	↔	↔	↔	↑↑↑↑	↑↑↑↑↑↑↑	↔	↔
IIB	↓	↓↓	↔	↔	↔	↓	↑↑↑↑	↑↑↑↑↑↑	↔	↔

Table 2: Summary of the effects of High Ca^{2+} (pCa 4.5; 30 mM Pi; pH 6.2) and Low Ca^{2+} (pCa 5.1; 30 mM Pi; pH 6.2) compared to Active (pCa 4.5; 5 mM Pi; pH 7.0) on F_0, number of Phase 3 observations, F_{SA}, $F_{SA}F_0$, and t_3 in MHC I, IIA, IIX, & IIB single muscle fibers. One arrow (↑,↓) in either direction represents a 15-20% change; ↔ represents no change; 0

5.2 Physiological Relevance

Our data suggests that for fast-contracting muscle fibers when fatigued and stretched, the same amount of myosin heads rebind to produce an F_{SA} like that of a stretch under Active. This is important because under fatiguing conditions SA is making a larger contribution towards specific tension production compared to Active, as demonstrated by F_{SA}/F_0. SA could play an important physiological role during repeated cyclical contractions by reducing the effect of fatigue on force production. As mentioned previously, an *in-vivo* example of such repeated cyclical contractions could be during locomotion (i.e., walking, jogging, or running). **Figure 20** depicts an individual during the swing phase of locomotion. As the right leg is being extended, the quadriceps (agonist) are contracting while the hamstrings (antagonist) are experiencing a stretch. During leg flexion the hamstrings are now the agonist muscle, applying a stretch to the quadriceps. As these muscles undergo repeated contraction-stretch patterns SA may become more relevant in the fast-contracting fibers as they begin to fatigue. This is especially promising since fast-contracting isoforms have been hypothesized to be more prone to fatigue compared to slow-contracting (47).

Figure 20: Model of a human undergoing locomotion. (Figure from Microsoft stock images)

5.3 Stretch Activation is lost in Slower-Contracting isoforms

MHC I and IIA fibers showed a strong SA response under Active conditions. However, in High Ca^{2+} Fatigue and Low Ca^{2+} Fatigue, MHC I fibers displayed no visible SA response (**Figure 19**), and MHC IIA fibers had an increased number of fibers showing no response from 20 to 75%, meaning no increase in force production above the expected decay in passive force due to stretch. Data that visually showed no SA response was well fit with two decaying exponentials, in other words, the third increasing exponential that is used to fit a normal stretch activation response wasn't needed.

The loss of SA under fatiguing conditions in slow contracting MHC I and IIA fibers only, with no loss in fast- and very fast-contracting MHC IIX and IIB fibers may be explained by differences in cross-bridge kinetics. There is evidence demonstrating differences in cross-bridge kinetics amongst MHC isoforms, including, but not limited to, the rate of myosin transition from weakly to strongly bound states ($2\pi b$) (54). Recent unpublished work from our lab also demonstrates muscle fatigue can influence $2\pi b$ in human single muscle fibers (25). **Figure 21** shows $2\pi b$ decreases from Control (Active, 14.7 ± 3.0) to Fatigue (High Ca^{2+} Fatigue, 9.4 ± 1.9) in MHC I and from 47.6 ± 4.9 to 38.8 ± 5.8 in MHC IIA fibers (please note, these are SD and not SE). Interestingly, while no pure MHC IIX isoforms were included, hybrid MHC IIAX fibers seemed to not experience as severe of a decline in $2\pi b$ under Fatigue as MHC I and IIA, possibly suggesting fiber-type differences of the effect of fatigue on cross-bridge kinetics. If we continue the general assumption that in response to a stretch Phase 2 is the result of myosin heads being ripped off actin while Phase 3 is myosin re-binding, then a slower weak-to-strong binding transition rate under fatigue could limit the number of heads able

to rebind when stretch. MHC I fibers already have the slowest r_3 under Active conditions (**Figure 18**), and this hypothetically would be expected to slow down even further under fatigue. MHC IIA fibers r_3 does slow down under fatigue, and even reaches similar values under Low Ca^{2+} Fatigue to that of MHC I fibers under Active. And with the possibility that faster isoforms may not experience the same level of $2\pi b$ drop-off under fatigue as slower MHC isoforms, the disappearance of a SA response in MHC I and IIA fibers under fatigue may ultimately be due to the myosin heads not being fast enough to rebind to actin in response to the stretch stimulus.

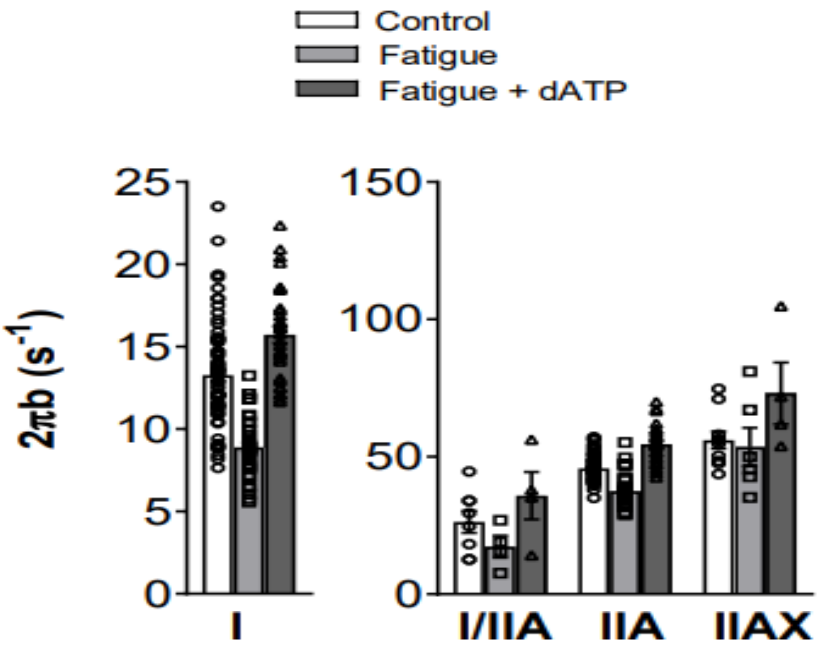

Figure 21: $2\pi b$ for maximal Ca^{2+}-activated (pCa 4.5) fibers for control, fatigue, and fatigue + dATP conditions by fiber type. $2\pi b$ is the rate of myosin transition between the weakly and strongly bound states. (25)

5.4 Comparison of Aims

Aim 1: Quantify F_{SA} during the initial, metabolite induced (Pi = 30 mM, pH = 6.2) stage of muscular fatigue in mouse soleus and EDL skeletal muscle fibers.

Hypothesis for Aim 1: F_{SA} will increase during the metabolic induced stage of fatigue in soleus (slow contracting) and decrease in EDL (fast contracting) skeletal muscle fibers compared to non-fatiguing conditions.

Analysis of Aim 1: F_{SA} increased from Active to High Ca^{2+} Fatigue for one (MHC IIA) of the two isoforms predominantly found in the soleus muscle. Interestingly, F_{SA} was similar between Active and High Ca^{2+} Fatigue for EDL fibers (MHC IIX & IIB), which was in opposition to our hypothesis.

Aim 2: Quantify F_{SA} during the secondary, Ca^{2+} induced stage of muscular fatigue and compare SA's potential role in modulating specific tension production between initial and secondary phases of muscular fatigue.

Hypothesis for Aim 2: F_{SA} will decrease in lower [Ca^{2+}] (secondary) fatigue conditions compared to the higher [Ca^{2+}] (initial) fatigue conditions for both soleus (slow contracting) and EDL (fast contracting) muscle fibers, with soleus fibers' F_{SA} being greater compared to EDL fibers' F_{SA} in lower [Ca^{2+}] (secondary) fatigue conditions.

Analysis of Aim 2: F_{SA} significantly decreased from High Ca^{2+} Fatigue to Low Ca^{2+} Fatigue in one (MHC IIB) of the two EDL fibers only. F_{SA} was similar between the two fatiguing conditions for MHC IIA (soleus) & IIX (soleus & EDL), however had a non-significant decreasing trend from High Ca^{2+} Fatigue to Low Ca^{2+} Fatigue. MHC IIA (soleus) and MHC IIX (mostly EDL) F_{SA} was similar between the two under Low Ca^{2+} Fatigue.

Discussion: The inspiration for the hypothesis for these aims were the findings from Straight et al. (76) (**Figure 7**). While a similar experimental apparatus was used,

there are a few key differences between Straight et al. and this study that need to be highlighted. First, only one component of muscular fatigue was investigated. As mentioned earlier, muscle fatigue is a complex issue that involves more than just the accumulation of Pi. At the molecular level, Pi and H^+ were shown to have distinct mechanisms on reducing myosin's force generation capability (87). Under acidosis (pH 6.4) and acidosis + Pi (30 mM) a similar decrease in force generation was observed. Acidosis saw force generation decline due to a decrease in the force per cross-bridge as well as an increase in negative force generating events (negative force refers to cross-bridges occurring in the opposite direction). However, when combined with 15 mM Pi (pH 6.4 + 15 mM Pi) the decline in force was due to the loss of high force generating events only, which the authors hypothesized to be the result of an increase in myosin detachment rate. The takeaway is that these two putative agents of muscle fatigue influence the cross-bridge cycle differently alone vs. in combination with one another. These differences could explain F_{SA} differing response between Straight et al. and our study, and we believe this to most likely culprit.

Other differences between the two studies, while most likely not driving the differences, need to be considered. Notably, the solutions used from Straight et al. were designed for *Drosophila* physiology, not mammalian. **Table 3** shows the difference in [constituents] for each Active solution for the two studies. Besides Pi, solutions differed in [ATP], pCa, [CP], [CPK], and ionic strength. ATP is the primary source of energy used during muscle contraction; pCa refers to $[Ca^{2+}]$; CP and CPK are responsible for maintaining adequate ATP supply; and ionic strength dictates the electrical field within the solution. All these differences could independently influence skeletal muscle

function, but importantly for this comparison is the difference in ionic strength. Higher ionic strength has been shown to impact muscle function, particularly by decreasing the number of force-generating cross-bridges (82). This could explain the difference in F_0 values seen between Straight et al. and this study. While not fully understood, this ionic strength difference could also influence the SA response.

The temperature in which the experiments were conducted differed as well. In Straight et al. both F_0 and F_{SA} were measured at 17°C, while in this study all experiments were conducted in 25°C. We have already gone into detail on how temperature can impact the kinetics of SA in **Section 2.2.5 Skeletal Muscle**.

Lastly, the samples used from Straight et al. were grouped based off muscle and not MHC isoform. Secondary analysis of the samples used from Straight et al. revealed five distinct isoforms used in their analysis, as shown in **Table 4**. The focus we placed on the loss of SA under fatiguing conditions was thanks to our relatively large MHC I sample size. Straight et al. had significantly less MHC I fibers included in their analysis, which may not have put this issue high on their radar. No MHC IIX fibers were collected, and most of the fast-contracting isoforms from the EDL muscle consisted of MHC IIB fibers. Since our study did not include hybrid isoforms, we cannot comment on what the F_{SA} response under fatigue would look like in these fewer common isoforms.

Chemical	Straight et al. (2019)	This Study
BES	20 mM	20 mM
EGTA	5 mM	5 mM
Mg^{2+}	1 mM	1 mM
DTT	1 mM	1 mM
Pi	varied	5 mM**
ATP	20 mM	5 mM**
CP	25 mM	15 mM**
CPK	450 units/mL	300 units/mL**
pCa	5.0	4.5**
Ionic Strength	260 mEq	175 mEq**

Table 3: List of constituents for the solutions used in both Straight et al. and this study. Differences are highlighted as '**'.

MHC Isoform	Straight et al. (2019)	Our Study
I	3	14
I/IIA	3	0
IIA	14	32
IIAX	0	0
IIX	0	11
IIXB	4	0
IIB	12	19

Table 4: MHC isoform distribution differences between the two studies. For Straight et al., all MHC I, I/IIA, and 13 of the 14 MHC IIA fibers were from the soleus muscle. For this study, all MHC I & IIA fibers came from soleus muscle. Five out of the 11 MHC IIX fibers came from the soleus, the rest from EDL. All 19 MHC IIB fibers were from the EDL. Analysis conducted by Philip Woods, winter of 2021.

5.4 Molecular Mechanism

As highlighted in **Section 2.3 Proposed Mechanisms of Stretch Activation**, several ideas on how muscle can generate F_{SA} have been proposed. Currently in the field, two prevailing mechanisms have grown in popularity to describe this phenomenon; the thin-filament based mechanism for cardiac and IFM and the myosin-based mechanism for skeletal muscle.

Thin-filament based mechanism. The thin-filament based involves the recruitment of "troponin-bridges", where myosin binds to troponin at sub-maximal [Ca^{2+}] and, in the presence of a stretch, mechanically tugs the troponin-tropomyosin complex freeing the initially blocked myosin binding sites. While this mechanism could occur in skeletal muscle, there are a few issues we must address. First, to our knowledge no one has investigated whether troponin-bridges can exist in vertebral muscle. Second, there are structural differences between IFM and vertebrate thin filaments. The spacing of troponin on the thin filament happens to coincide with the spacing of cross-bridges on the thick filament in IFM, which is not the case in vertebrate (10). Also, IFM contain predominately two TnC isoforms, TnC1 and TnC4, with TnC4 seeming critical for F_{SA} generation (33). Vertebrate muscle, on the other hand, contains sTnC and cTnC isoforms for slow- and fast-contracting muscle (32). Lastly, if we assume that troponin-bridges do exist in vertebral muscle, then under Low Ca^{2+} Fatigue more myosin binding sites would in theory be blocked on actin, and we would hypothesize that troponin-bridges would have a higher probability of occurring. This could then increase the proportion of myosin binding sites able to be mechanically tugged free, producing a larger F_{SA} under Low Ca^{2+} Fatigue compared to High Ca^{2+} Fatigue. Our data, however, does not support such a

possibility. There is, however, conflicting evidence suggesting peak F_{SA} occurs either at sub-maximal or maximal [Ca^{2+}] in IFM (33), which could alter our assumptions.

Myosin-based mechanism. The myosin-based mechanism states that in the presence of moderate Pi and a stretch, some of the strongly bound post-power stroke cross-bridges rebind with Pi and are forced back into the weakly bound, pre-power stroke state. The reversal of weak-to-strong bounding can repeat the cross-bridge cycle without having to hydrolyze a new ATP molecule and produce F_{SA}. In theory, the higher the [Pi] the greater probability of this reversal, which leads to a greater probability of cross-bridges rebinding and redoing the power stroke. We believe our data fits more accurately within this mechanism.

Referring to **Figure 9A**, we propose from the results of this study that the green arrow is occurring under all three conditions (Active, High Ca^{2+} Fatigue and Low Ca^{2+} Fatigue). Under Active conditions, high amounts of strong-binding events are occurring, meaning high levels of myosin-actin interactions that some of which could undergo the green arrow when stretched to produce F_{SA}. Under High Ca^{2+} Fatigue, due to most likely elevated Pi and H^+, we propose the green arrow to be occurring more frequently. However, since these fatiguing agents decrease strong-binding events, the increased frequency of F_{SA} is limited to the number of myosin-actin interactions, which could explain the similar F_{SA} values under Active and High Ca^{2+} Fatigue observed in this study. The decline in [Ca^{2+}] under Low Ca^{2+} Fatigue would further reduce strong-binding events by increasing tropomyosin blockage. This could, in theory, increase the proportion of myosin weak binding, creating an environment of myosin heads close to the thin filament

ready to benefit from the stretch stimulus. This proposed mechanistic explanation is fully exploratory and requires further investigation.

5.5 Limitations and Future Directions

There are several limitations to this study. First, while the experimental conditions are representative of *in-vivo* fatigue and give insight into whether this phenomenon may be physiologically relevant, determining exactly which metabolic condition (Pi, H^+, Ca^{2+}) is driving these changes (or lack thereof) proves difficult. Future studies should investigate Pi alone, H^+ alone, and Pi in combination with H^+ effect on the SA response within mammalian skeletal muscle. Second, the magnitude of stretch was 0.5% ML for all conditions. Larger stretches should in theory produce a larger SA response, and under fatigue larger stretches may be required to elicit SA for slower-contracting isoforms. This phenomenon should also be investigated in other vertebral skeletal muscles, particularly in human subjects, as we proposed this could benefit human locomotion. Last, while F_{SA} was determined as described in **Section 3.4 Analysis of Stretch Activation**, the range at which SA occurs is selected by the user, which introduces a certain degree of bias. Moving forward, researchers investigating SA need to design a more automated approach to investigating the phenomenon that controls user bias. One such approach could be the use of the changepoint() function in R.

5.6 Conclusion

This study provided a novel insight into stretch activation (SA) within mammalian skeletal muscle. Simulated muscle fatigue, both at the initial (30 mM Pi, pH 6.2) and secondary (30 mM Pi, pH 6.2, pCa 5.1) reduced calcium-activated specific tension (F_0) while having minimal to no change in stretch activated specific tension (F_{SA})

in fast-contracting single muscle fibers. This left the ratio of stretch-to-calcium activated specific tension (F_{SA}/F_0) high under both fatiguing conditions compared to Active, demonstrating SA as significant modulator of specific tension production under fatigue conditions. Slow-contracting isoforms demonstrated no SA under fatiguing conditions, further exacerbating SA being fiber-type dependent. By understanding SA under fatigue, we have now demonstrated a new possible mechanism for reducing the declines in force generation for prolonged locomotion. Future work should focus on investigating in what type of locomotion, whether walking, jogging, or running, SA could serve most beneficial.

BIBLIOGRAPHY

1. **Aidley BDJ**, **White DCS**. Mechanical Properties of Glycerinated Fibres from the tymbal muscles of a brazilian cicada. .

2. **Allen D**, **Lannergren J**, **Westerblad H**. Muscle cell function during prolonged activity: cellular mechanisms of fatigue. *Exp Physiol* 80: 497–527, 1995. doi: 10.1113/expphysiol.1995.sp003864.

3. **Allen DG**, **Clugston E**, **Petersen Y**, **Röder I V.**, **Chapman B**, **Rudolf R**. Interactions between intracellular calcium and phosphate in intact mouse muscle during fatigue. *J Appl Physiol* 111: 358–366, 2011. doi: 10.1152/japplphysiol.01404.2010.

4. **Allen DG**, **Lamb GD**, **Westerblad H**. Skeletal muscle fatigue: Cellular mechanisms. *Physiol Rev* 88: 287–332, 2008. doi: 10.1152/physrev.00015.2007.

5. **Augusto V**, **Padovani CR**, **Eduardo G**, **Campos R**. Skeletal Muscle Fiber Types in C57BL6J Mice. 21: 89–94, 2004.

6. **Bárány M**. ATPase activity of myosin correlated with speed of muscle shortening. *J Gen Physiol* 50, 1967. doi: 10.1085/jgp.50.6.197.

7. **Boettiger EG**. The machinery of insect flight. *Univ. Orgeon Publ.*: 117–142, 1957.

8. **Bottinelli R**, **Schiaffino S**, **Reggiani C**. Force-Velocity Relations And Myosin Heavy Chain Isoform Compositions of Skinned Fibres From Rat Skeletal Musscle.

9. **Broxterman RM**, **Layec G**, **Hureau TJ**, **Amann M**, **Richardson RS**. Skeletal muscle bioenergetics during all-out exercise: mechanistic insight into the oxygen uptake slow component and neuromuscular fatigue. *J Appl Physiol* 122: 1208–1217, 2017. doi: 10.1152/japplphysiol.01093.2016.-Although.

10. **Bullard B**, **Pastore A**. Regulating the contraction of insect flight muscle. *J Muscle Res Cell Motil* 32: 303–313, 2011. doi: 10.1007/s10974-011-9278-1.

11. **Campbell KB**, **Chandra M**. Functions of Stretch Activation in Heart Muscle. *J Gen Physiol J Gen Phys* 127: 89–94, 2006. doi: 10.1085/jgp.200509483.

12. **Cooke R**. Modulation of the actomyosin interaction during fatigue of skeletal muscle. *Muscle and Nerve* 36: 756–777, 2007. doi: 10.1002/mus.20891.

13. **D'Antona G**, **Lanfranconi F**, **Pellegrino MA**, **Brocca L**, **Adami R**, **Rossi R**, **Moro G**, **Miotti D**, **Canepari M**, **Bottinelli R**. Skeletal muscle hypertrophy and structure and function of skeletal muscle fibres in male body builders. *J Physiol* 570: 611–627, 2006. doi: 10.1113/jphysiol.2005.101642.

14. **Daniel TL**, **Trimble AC**, **Chase PB**. Compliant realignment of binding sites in muscle: Transient behavior and mechanical tuning. *Biophys J* 74: 1611–1621, 1998. doi: 10.1016/S0006-3495(98)77875-0.

15. **Debold EP**. Recent insights into the molecular basis of muscular fatigue. *Med Sci Sports Exerc* 44: 1440–1452, 2012. doi: 10.1249/MSS.0b013e31824cfd26.

16. **Debold EP**. Decreased Myofilament Calcium Sensitivity Plays a Significant Role in Muscle Fatigue. *Exerc Sport Sci Rev* 44: 144–149, 2016. doi: 10.1249/JES.0000000000000089.

17. **Debold EP**, **Romatowski J**, **Fitts RH**. The depressive effect of Pi on the force-pCa relationship in skinned single muscle fibers is temperature dependent. *Am J Physiol - Cell Physiol* 290, 2006. doi: 10.1152/ajpcell.00342.2005.

18. **Dickinson MH**, **Hyatt CJ**, **Lehmann FO**, **Moore JR**, **Reedy MC**, **Simcox A**, **Tohtong R**, **Vigoreaux JO**, **Yamashita H**, **Maughan DW**. Phosphorylation-dependent power output of transgenic flies: An integrated study. *Biophys J* 73: 3122–3134, 1997. doi: 10.1016/S0006-3495(97)78338-3.

19. **Dudley R**. Comparative Biomechanics and the Evolutionary Diversification of Flying Insect Morphology. In: *Functional Morphology, Biomechanics, and Evolutionary Process*. 1991, p. 503–514.

20. **Eldred CC**, **Katzemich A**, **Patel M**, **Bullard B**, **Swank DM**. The roles of troponin C isoforms in the mechanical function of Drosophila indirect flight muscle. *J Muscle Res Cell Motil* 35: 211–223, 2014. doi: 10.1007/s10974-014-9387-8.

21. **Engel WK**. The essentially of histo- and cytochemical studies muscle in the investigation of neuromuscular disease. *Neurology* 12: 771–794, 1962. doi: 10.1212/wnl.51.3.655.

22. **Fabiato A**, **Fabiato F**. Effects of pH on the myofilaments and the sarcoplasmic reticulum of skinned cells from cardiace and skeletal muscles. *J Physiol* 276: 233–255, 1978. doi: 10.1113/jphysiol.1978.sp012231.

23. **Fitts RH**. The cross-bridge cycle and skeletal muscle fatigue. *J Appl Physiol* 104: 551–558, 2008. doi: 10.1152/japplphysiol.01200.2007.

24. **Ford LE**, **Huxley AF**, **Simmons RM**. Tension responses. *J Physiol* 269: 441–515, 1977.

25. **Foster A**. Mechanisms and Mitigation of Skeletal Muscle Fatigue in Single Fibers from Older Adults [Online]. University of Massachusetts Amherst: 2019. https://scholarworks.umass.edu/masters_theses_2.

26. **Fukuda N**, **Wu Y**, **Farman G**, **Irving TC**, **Granzier H**. Titin-based modulation of active tension and interfilament lattice spacing in skinned rat cardiac muscle. *Pflugers Arch Eur J Physiol* 449: 449–457, 2005. doi: 10.1007/s00424-004-1354-6.

27. **Galler, S.; Schmitt, TL.; Hilber, K.; Pette D**. Stretch activation and isoforms of myosin heavy chain and troponin-T of rat skeletal muscle fibres. *J Muscle Res Cell Motil* 18: 555–561, 1997.

28. **Galler S**. Stretch activation of skeletal muscle fibre types. .

29. **Galler S**, **Hilber K**, **Pette D**. Stretch activation and myosin heavy chain isoforms of rat, rabbit and human skeletal muscle fibres. *J Muscle Res Cell Motil* 18: 441–448, 1997. doi: 10.1023/A:1018646814843.

30. **Galler S**, **Schmitt T**, **Pette D**. Stretch activation, unloaded shortening velocity, and myosin heavy chain isoforms of rat skeletal muscle fibres. .

31. **Galler S**, **Schmitt TL**, **Hilber K**, **Pette D**. Stretch activation and isoforms of myosin heavy chain and troponin-T of rat skeletal muscle fibres. *J Muscle Res Cell Motil* 18: 555–561, 1997.

32. **Gillis TE**, **Marshall CR**, **Tibbits GF**. Functional and evolutionary relationships of troponin C. *Physiol Genomics* 32: 16–27, 2007. doi: 10.1152/physiolgenomics.00197.2007.

33. **Glasheen BM**, **Eldred CC**, **Sullivan LC**, **Zhao C**, **Reedy MK**, **Edwards RJ**, **Swank DM**. Stretch activation properties of Drosophila and Lethocerus indirect flight muscle suggest similar calcium-dependent mechanisms. *Am J Physiol Cell Physiol* 313: C621–C631, 2017. doi: 10.1152/ajpcell.00110.2017.

34. **Godt RE**, **Lindley BD**. Influence of temperature upon contractile activation and isometric force production in mechanically skinned muscle fibers of the frog. *J Gen Physiol* 80: 279–297, 1982. doi: 10.1085/jgp.80.2.279.

35. **Granzier HLM**, **Wang K**. Interplay between passive tension and strong and weak binding cross-bridges in insect indirect flight muscle: A Functional Dissection by Gelsolin-mediated Thin Filament Removal. *J Gen Physiol* 101: 235–270, 1993. doi: 10.1085/jgp.101.2.235.

36. **Hamalainen, Nina.; Pette D**. Patters of myosin isoforms in mamalian skeletal muscle fibres. *Microsc Res Tech* 30, 1995.

37. **Heinl, P.; Kuhn, H.J.; Ruegg JC**. Tension responses to quick length changes of glycerinated skeletal muscle fibres from the frog and toroise. *J Physiol* 237: 243–258, 1974.

38. **Heinl P**. Mechanische Aktivierung und Deaktivierung der isolierten contractilen Struktur des Froschsartorius durch rechteckf6rmige und sinusfgrmige L/ingen/inderungen. .

39. **Hu Z**, **Taylor DW**, **Reedy MK**, **Edwards RJ**, **Taylor KA**. Structure of myosin filaments from relaxed Lethocerus flight muscle by cryo-EM at 6 Å resolution. *Sci Adv* 2, 2016. doi: 10.1126/sciadv.1600058.

40. **Huxley AF**, **Simmons RM**. Proposed mechanism of force generation in striated muscle. *Nature* 233: 533–538, 1971. doi: 10.1038/233533a0.

41. **Jewell, B.R.; Ruegg JC**. Oscillatory contraction of insect fibrillar muscle after glycerol extraction. *Proc R Soc London Ser B Biol Sci* 164: 428–459, 1966. doi: 10.1098/rspb.1966.0042.

42. **Josephson RK**, **Malamud JG**, **Stokes DR**. Asynchronous muscle: A primer. *J Exp Biol* 203: 2713–2722, 2000.

43. **Josephson RK**, **Malamud JG**, **Stokes DR**. Power output by an asynchronous flight muscle from a beetle. *J Exp Biol* 203: 2667–2689, 2000. doi: 10.1242/jeb.203.17.2667.

44. **Julian FJ**, **Sollins MR**. Variation of muscle stiffness with force at increasing speeds of shortening. *J Gen Physiol* 66: 287–302, 1975. doi: 10.1085/jgp.66.3.287.

45. **Kawai, M.; Brandt PW**. resting stiffness and tension of stretched crayfish muscle fibers. .

46. **Kent-Braun JA**. Central and peripheral contributions to muscle fatigue in humans during sustained maximal effort. *Eur J Appl Physiol Occup Physiol* 80: 57–63, 1999. doi: 10.1007/s004210050558.

47. **Kent-Braun JA**, **Fitts RH**, **Christie A**. Skeletal muscle fatigue. *Compr Physiol* 2: 997–1044, 2012. doi: 10.1002/cphy.c110029.

48. **Lee JA**, **Westerbladt H**, **Allent DG**. Changes in tetanic and resting [Ca2+] during fatigue and recovery of single muscle fibres from xenopus laevis. : 307–326, 1991.

49. **Linari, Marco.; Reedy, Michael K.; Reedy, Mary C.; Lombardi, Vincenzo.; Piazzesi G**. Ca-Activation and Stretch-Activation in Insect Flight Muscle. *Biophys J* 87: 1101–1111, 2004.

50. **Longyear TJ**, **Turner MA**, **Davis JP**, **Lopez J**, **Biesiadecki B**, **Debold EP**. Ca++-sensitizing mutations in troponin, Pi, and 2-deoxyATP alter the depressive effect of acidosis on regulated thin-filament velocity. *J Appl Physiol* 116: 1165–1174, 2014. doi: 10.1152/japplphysiol.01161.2013.

51. **Loya AK**, **Houten SK Van**, **Glasheen BM**, **Swank DM**. *Shortening deactivation : quantifying a critical component of cyclical muscle contraction*. [date unknown].

52. **Martyn DA**, **Chase PB**, **Regnier M**, **Gordon AM**. A simple model with myofilament compliance predicts activation-dependent crossbridge kinetics in skinned skeletal fibers. *Biophys J* 83: 3425–3434, 2002. doi: 10.1016/S0006-3495(02)75342-3.

53. **Millar NC**, **Homsher E**. The effect of phosphate and calcium on force generation in glycerinated rabbit skeletal muscle fibers. A steady-state and transient kinetic study. *J Biol Chem* 265: 20234–20240, 1990. doi: 10.1016/s0021-9258(17)30494-5.

54. **Miller MS**, **Bedrin NG**, **Ades PA**, **Palmer BM**, **Toth MJ**. Molecular determinants of force production in human skeletal muscle fibers: Effects of myosin isoform expression and cross-sectional area. *Am J Physiol - Cell Physiol* 308: C473–C484, 2015. doi: 10.1152/ajpcell.00158.2014.

55. **Miller MS**, **Bedrin NG**, **Callahan DM**, **Previs MJ**, **Jennings ME**, **Ades PA**, **Maughan DW**, **Palmer BM**, **Toth MJ**. Age-related slowing of myosin actin cross-bridge kinetics is sex specific and predicts decrements in whole skeletal muscle performance in humans. *J Appl Physiol* 115: 1004–1014, 2013. doi: 10.1152/japplphysiol.00563.2013.

56. **Miller MS**, **VanBuren P**, **LeWinter MM**, **Braddock JM**, **Ades PA**, **Maughan DW**, **Palmer BM**, **Toth MJ**. Chronic heart failure decreases cross-bridge kinetics in single skeletal muscle fibres from humans. *J Physiol* 588: 4039–4053, 2010. doi: 10.1113/jphysiol.2010.191957.

57. **Moore JR**. Stretch Activation: toward a molecular mechanism. 2005.

58. **Nelson CR**, **Fitts RH**. Effects of low cell pH and elevated inorganic phosphate on the pCa-force relationship in single muscle fibers at near-physiological temperatures. *Am J Physiol - Cell Physiol* 306: 670–678, 2014. doi: 10.1152/ajpcell.00347.2013.

59. **Palmer S**, **Kentish JC**. The role of troponin C in modulating the Ca2+ sensitivity of mammalian skinned cardiac and skeletal muscle fibres. *J Physiol* 480: 45–60, 1994. doi: 10.1113/jphysiol.1994.sp020339.

60. **Parsons B**, **Szczesna D**, **Zhao J**, **Van Slooten G**, **Kerrick WGL**, **Putkey JA**, **Potter JD**. The effect of pH on the Ca2+ affinity of the Ca2+ regulatory sites of skeletal and cardiac troponin C in skinned muscle fibres. *J Muscle Res Cell Motil* 18: 599–609, 1997. doi: 10.1023/A:1018623604365.

61. **Peckham, M.; Molloy, J.E.; Sparrow, J.C.; White DCS**. Physiological properties of the dorsal longitudinal flight muscle and the tergal depressor of the trochanter muscle of Drosophila melanogaster. .

62. **Perz-Edwards RJ**, **Irving TC**, **Baumann BAJ**, **Gore D**, **Hutchinson DC**, **Kržič U**, **Porter RL**, **Ward AB**, **Reedy MK**. X-ray diffraction evidence for myosin-troponin connections and tropomyosin movement during stretch activation of insect flight muscle. *Proc Natl Acad Sci U S A* 108: 120–125, 2011. doi: 10.1073/pnas.1014599107.

63. **Pette D**, **Staron RS**. Cellular and molecular diversities of mammalian skeletal muscle fibers. 1990.

64. **Pringle J**. The Excitation and Contraction of the Flight Muscles of Insects. .

65. **Pringle J**. The Croonian Lecture. Stretch activation of muscle: function and mechanism. 1977, p. 108–130.

66. **Rivero JLL**, **Talmadge RJ**, **Edgerton VR**. Correlation between myofibrillar ATPase activity and myosin heavy chain composition in equine skeletal muscle and the influence of training. *Anat Rec* 246: 195–207, 1996. doi: 10.1002/(SICI)1097-0185(199610)246:2<195::AID-AR6>3.0.CO;2-0.

67. **Roeder KD**. Movements of the thorax and potential changes in the thoracic muscles of insects during flight. .

68. **Ruegg, J.C.; Steiger, G.J.; Schadler M**. Mechanical Activation of the Contractile System in Skeletal Muscle. .

69. **Schneider CA**, **Rasband WS**, **Eliceiri KW**. NIH Image to ImageJ: 25 years of image analysis. *Nat Methods* 9: 671–675, 2012. doi: 10.1038/nmeth.2089.

70. **Scott W**, **Stevens J**, **Binder-Macleod SA**. Human skeletal muscle fiber type classifications. *Phys Ther* 81: 1810–1816, 2001. doi: 10.1093/ptj/81.11.1810.

71. **Steiger G**. *Stretch Activation and Myogenic Oscillation of Isolated Contractile Structures of Heart Muscle**. Springer-Verlag, 1971.

72. **Steiger G**. Stretch activation and tension transients in cardiac, skeletal and insect flight muscle. In: *Insect Flight Muscle*. 1977, p. 221–268.

73. **Stelzer JE**, **Brickson SL**, **Locher MR**, **Moss RL**. Role of myosin heavy chain composition in the stretch activation response of rat myocardium. *J Physiol* 579: 161–173, 2007. doi: 10.1113/jphysiol.2006.119719.

74. **Stelzer JE**, **Dunning SB**, **Moss RL**. Ablation of Cardiac Myosin-Binding Protein-C Accelerates Stretch Activation in Murine Skinned Myocardium. .

75. **Stienen GJM**. Chronicle of skinned muscle fibres. *J Physiol* 527: 1, 2000. doi: 10.1111/j.1469-7793.2000.t01-2-00001.x.

76. **Straight CR**, **Bell KM**, **Slosberg JN**, **Miller MS**, **Swank DM**. A myosin-based mechanism for stretch activation and its possible role revealed by varying phosphate concentration in fast and slow mouse skeletal muscle fibers. *Am J Physiol - Cell Physiol* 317: C1143–C1152, 2019. doi: 10.1152/ajpcell.00206.2019.

77. **Swank DM**. Mechanical analysis of Drosophila indirect flight and jump muscles. *Methods* 56: 69–77, 2012. doi: 10.1016/j.ymeth.2011.10.015.

78. **Syme DA**, **Josephson RK**. Influence of muscle length on work from trabecular muscle of frog atrium and ventricle. *J Exp Biol* 198: 2221–2227, 1995. doi: 10.1242/jeb.198.10.2221.

79. **Thorson J**, **White DCS**. Distributed Representations for Actin-Myosin Interaction in the Oscillatory Contraction of Muscle. *Biophys J* 9: 360–390, 1969. doi: 10.1016/S0006-3495(69)86392-7.

80. **Tolwinski NS**. Introduction: Drosophila-A model system for developmental biology. *J Dev Biol* 5: 10–11, 2017. doi: 10.3390/jdb5030009.

81. **Unger M**, **Debold EP**. Acidosis decreases the Ca2+ sensitivity of thin filaments by preventing the first actomyosin interaction. *Am J Physiol - Cell Physiol* 317: C714–C718, 2019. doi: 10.1152/ajpcell.00196.2019.

82. **Wang L**, **Bahadir A**, **Kawai M**. High ionic strength depresses muscle contractility by decreasing both force per cross-bridge and the number of strongly attached cross-bridges. 2015.

83. **Westerblad, Håkau.; Allen DG**. Changes of myoplasmic calcium concentration during fatigue in single mouse muscle fibers. *J Gen Physiol* 98, 1991.

84. **Westerblad, Håkau.; Allen DG**. Emerging roles of ROS/RNS in muscle function and fatigue. *Antioxid Redox Signal* 15, 2011.

85. **Westerblad BYH**, **Allen DG**. Fatigued Single Fibres From Mouse Skeletal Muscle. : 729–740, 1993.

86. **Wood DS**, **Zollman J**, **Reuben JP**, **Brandt PW**. Human skeletal muscle: Properties of the "chemically skinned" fiber. *Science (80-)* 187: 1075–1076, 1975. doi: 10.1126/science.187.4181.1075.

87. **Woodward M**, **Debold EP**. Acidosis and phosphate directly reduce myosin's force-generating capacity through distinct molecular mechanisms. *Front Physiol* 9: 1–6, 2018. doi: 10.3389/fphys.2018.00862.

88. **Wray JS**. Filament geometry and the activation of insect flight muscles. *Nature* 280, 1979.

89. **Wu S**, **Liu J**, **Reedy MC**, **Tregear RT**, **Winkler H**, **Franzini-Armstrong C**, **Sasaki H**, **Lucaveche C**, **Goldman YE**, **Reedy MK**, **Taylor KA**. Electron tomography of cryofixed, isometrically contracting insect flight muscle reveals novel actin-myosin interactions. *PLoS One* 5: 1–21, 2010. doi: 10.1371/journal.pone.0012643.

90. **Zhao C**, **Swank DM**. An embryonic myosin isoform enables stretch activation and cyclical power in Drosophila jump muscle. *Biophys J* 104: 2662–2670, 2013. doi: 10.1016/j.bpj.2013.04.057.

91. **Zhao C**, **Swank DM**. The Drosophila indirect flight muscle myosin heavy chain isoform is insufficient to transform the jump muscle into a highly stretch-ctivated muscle type. *Am J Physiol - Cell Physiol* 312: C111–C118, 2017. doi: 10.1152/ajpcell.00284.2016.